South African Journal of Chemical Engineering 54 (2025) 114–132

Contents lists available at ScienceDirect

South African Journal of Chemical Engineering

journal homepage: www.elsevier.com/locate/sajce

Investigation of toluene alkylation with hept-1-ene over fresh and modified h-beta catalysts according to apparent activation energy values

Ali Al-Shathr [a], Bashir Y. Al-Zaidi [b], Safa Aal-Kaeb [c], Zaidoon M. Shakor [a], Hasan Sh. Majdi [d], May A. Alsaffar [c], Muhannad A.E. Al-Saedy [e], Ahmed Majeed Jassem [f], Ramzy S. Hamied [g], Firas K. Al-Zuhairi [a], Adnan A. AbdulRazak [c], Talib M. Albayati [a,*], James McGregor [h]

[a] Department of Petroleum Refining and Gas Technology Engineering, College of Chemical Engineering, University of Technology- Iraq, Baghdad 10066, Iraq
[b] Department of Chemical Process Engineering, College of Chemical Engineering, University of Technology- Iraq, Baghdad 10066, Iraq
[c] Department of Chemical Engineering and Petroleum Pollution, College of Chemical Engineering, University of Technology- Iraq, Baghdad 10066, Iraq
[d] Chemical Engineering and Oil Refinery Department, AlMustaqbal University College, Hilla, Babylon, Iraq
[e] Department of Chemistry, Mustansiriyah University, Baghdad, Iraq
[f] Department of Chemistry, College of Education for Pure Sciences, University of Basrah, Basrah, Iraq
[g] College of Petroleum Technology, University of Technology- Iraq, Baghdad 10066, Iraq
[h] School of Chemical, Materials and Biological Engineering, University of Sheffield, Sheffield S1 3JD, United Kingdom

ARTICLE INFO

Keywords:
Toluene alkylation
Double-bond isomerisation
Coke formation
Kinetic modelling
Dealuminated and desilicated

ABSTRACT

This work has demonstrated improved conversion and selectivity and reduced coking in the alkylation of toluene with hept-1-ene to linear alkyl methyl benzenes over onto H-beta (Si/Al = 367), desilicated H-beta (Si/Al = 231) and dealuminated H-beta (Si/Al = 563) zeolite catalysts. Additionally, kinetic modelling provided support for the proposed reaction mechanism, facilitating the design of improved catalysts for this reaction. The production of linear alkyl methyl benzenes is of critical import in the manufacture of detergents, a rapidly growing sector globally, however currently processes are limited by catalyst deactivation as a result of coke deposition. The properties of the parent and modified catalysts were analysed using XRD, FTIR, SEM, ICP-AES, TGA, and BET surface area. The results indicate that both types of catalysts whose structural framework was modified *via* acid or base leaching treatment techniques had improved catalytic activity, leading to an enhancement in the conversion and selectivity towards double-bond isomerisation and alkylation products. In addition, the experimental results were fitted using a reaction scheme consisting of seven components and thirteen reactions. Nonlinear optimization (genetic algorithm technique) with numerical integration (4th order Runge-Kutta) was utilized to predict the kinetic parameters, while Matlab 2021a software was used to perform all computation. The mean relative errors (MRE) values estimated from comparing experimental and model-predicted outcome data showed remarkable agreement.

1. Introduction

During 2020, economic growth suffered negative effects due to the Covid-19 pandemic sweeping almost all parts of the world, and this led to an increase in hygiene awareness campaigns, which caused an increase in global demand for linear alkyl methyl benzene, which is the main raw material in the production of detergents [Chaurasia et al., 2022, Mulakhudair et al., 2023]. Linear alkyl benzene production in 2020 amounted to about 3.5 kilotons and is expected to rise to about 4 kilotons by 2026 with an annual growth rate of about 3 % [Mordor-Intelligence 2023]. Interest in linear alkyl methylbenzene began in the 1960s when it replaced dodecylbenzene in detergent industries because it has high biodegradability, is environmentally friendly, and is cost effective [Lovás et al., 2014, Kocal et al., 2001]. It is produced either through the alkylation of benzene or toluene with alpha olefins using aluminium chloride or through the use of hydrofluoric acid as a homogeneous catalyst [S.H. Al-Sultani et al., 2024, Gunnoe et al., 2020]. However, due to the frequent problems resulting from the use of a homogeneous catalyst, a heterogeneous catalyst was used instead such as zeolite because it has high activity and stability throughout the reaction [Vogt and Weckhuysen, 2022, Gomez and al., 2020,

* Corresponding author.
E-mail address: talib.m.naieff@uotechnology.edu.iq (T.M. Albayati).

https://doi.org/10.1016/j.sajce.2025.07.010
Received 10 January 2025; Received in revised form 27 May 2025; Accepted 27 July 2025
Available online 28 July 2025

Nomenclatures and abbreviations

C_i	i^{th} reactant concentration (mol/m^3)
E	Activation energies (kJ/mol)
E_a	Apparent activation energies (kJ/mol)
N	Number of components (-)
MAE	Mean absolute error (-)
MRE	Mean relative error (-)
M	Number of experiments (-)
T	Time (min)
r_j	j^{th} reaction rate and j is the reaction number (mol/gm cat. Min)
V	Reactor volume (m^3)
W_c	Weight of catalyst (gm)
$y_{i,k}^{exp}$	Experimental weight fraction (-)
$y_{i,k}^{pred}$	Predicted weight fraction (-)
$a_{i,j}$	The reactant i stoichiometric ratio within reaction j (-)

Quintana-Gómez et al., 2022, Intang et al., 2024]. The use of heterogeneous catalysts facilitates the procedures for separating the spent catalyst (i.e., deactivated catalyst) after the end of the reaction and then reactivating it for the purpose of using it in the subsequent reaction, thus reducing the overall cost of the process [Ali et al., 2023, van Vreeswijk et al., 2023]. However, deactivation remains the major drawback of the use of heterogeneous catalyst [Yuan and al., 2023, Shakor and Shafei, 2023].

Beta zeolite is a high-silica framework, having a large pore aperture of about 7.6 Å with 12-membered 3D rings [Liu et al., 2022, Zaykovskaya et al., 2020, Hong et al., 2023]. It is also characterized by its high thermal stability, which makes it one of the important zeolite catalysts in hydrocarbon reactions. In its structural framework, H-beta contains a large channel that makes it suitable for alkylation and isomerisation reactions. In fact, several factors play a vital role to reduce the deactivation effect, such as catalyst acidity, pore structure, nature and location of the coke, silica to alumina ratio, and other operating conditions [Díaz et al., 2021]. Therefore, zeolite modification techniques have become the main requirement to overcome deactivation problems and hence increase the yield of alkylation products at a lower cost. Dealumination and/or desilication are the most important post-synthesis treatments currently employed to modify the structure of the zeolite catalyst through acid leaching and/or base leaching [Imyen et al., 2020].

On the one hand, dealumination involves chemical and structural modification of zeolite by removing aluminium atoms from its lattice [Yoshioka et al., 2022]. In fact, the ratio of silica to alumina (Si/Al) is the main factor affecting the properties of zeolite such as acidity, thermal stability and selectivity. Removal of aluminium from the zeolite structure increases the value of the Si/Al ratio and also decreases the acidic sites within it [Silaghi et al., 2014]. During the reaction, zeolites become more stable when the value of the Si/Al ratio increases because this slows down the deactivation process. However, a mesoporous structure may form as a result of the removal of aluminium atoms, leading to the formation of some vacancies. In general, dealumination modification of H-beta zeolite is easier than other high-silica zeolites such as H-ZSM-5 due to the presence of stacking defects [Müller et al., 2000]. The crystallinity of zeolite decreases after dealumination modification procedure, and this can be proven by comparing the X-ray diffraction patterns of the treated zeolite sample with the parent sample [Mendoza Merlano et al., 2022, Adriano et al., 2022, Ilcheva et al., 2024, Nisar et al., 2024]. Minami et al., [Minami et al., 2022] showed that beta zeolite had a Si/Al ratio value of 12.2 after being treated by acid leaching *via* H_2SO_4. This value increased to 70 without a collapse within its framework structure and without a radical change in its crystallographic structure. Boveri et al., [Boveri et al., 2006] utilized mordenite zeolite with a Si/Al value of 9.5 to study the effect of dealumination modification on its catalytic behaviour in benzene alkylation reactions with 1-dodecene. They found that the value of the Si/Al ratio increased to around 18 with a noticeable improvement in its catalytic activity and high selectivity towards the desired product due to the increased conversion of 1-dodecene compared to the catalytic activity of fresh mordenite zeolite. It was also observed that the coke rate decreased as a result of the formation of mesoporous during the treatment of the catalyst with acid.

Desilication is a subsequent chemical treatment after the initial preparation of the catalyst and is carried out by dissolution of silicon atoms (i.e., the secondary-building units or SBUs) from zeolite framework in an aqueous alkaline solution. The purpose is to produce a new structural composition of zeolite containing a distribution of micropores and mesopores and this is usually done through the use of basic media, such as sodium hydroxide [Přech et al., 2018, K. Zhang et al., 2018]. According to the formation of mesopores within the structure of the zeolite catalyst after removing part of the lattice silicon atoms, its hierarchical features are improved throughout the reaction such as easy access to the active acid sites, enhanced thermal stability, reducing the amount of coke accumulated, and the mass transfer of bulk products becomes faster as well [Wang et al., 2022, Aziz et al., 2023]. It should be noted that the value of the Si/Al ratio is a critical factor that can fundamentally affect the desilication modification and thereby affect the formation of mesopores and increase the opening of the structural composition of the zeolite catalyst [Singh et al., 2021]. Aslam et al. [Aslam et al., 2014] investigated the effect of treating the catalyst *via* desilication and its impact on both activity and selectivity by studying the alkylation of benzene with 1-dodecene using mordenite and beta zeolites. They concluded that mordenite zeolite showed higher 1-dodecene conversion and greater 2-dodecylbenzene selectivity compared to beta zeolite. Moreover, the mass transfer rate of products on the surface of desilicated zeolite is better than that of fresh zeolite, which means that the thermal stability becomes high after treatment, and this leads to increased life of the zeolite and reduced possibility of deactivation during the reaction. In addition to the above, Lu and his co-workers indicated the effect of the modified beta-type zeolite structure on its catalytic behaviour through alkylation of benzene with 1-dodecene [Lu et al., 2021]. They found that beta mesopore zeolite is more stable than fresh beta zeolite and obtained better diffusivity by using mesopore zeolite. This enhances the possibility of improving the activity and selectivity of bilinear alkyl benzene on its surface. In fact, three isomers of linear heptyl-methylbenzene, namely 2-, 3-, and 4-heptyl-methylbenzene, are obtained through the alkylation reaction of toluene with

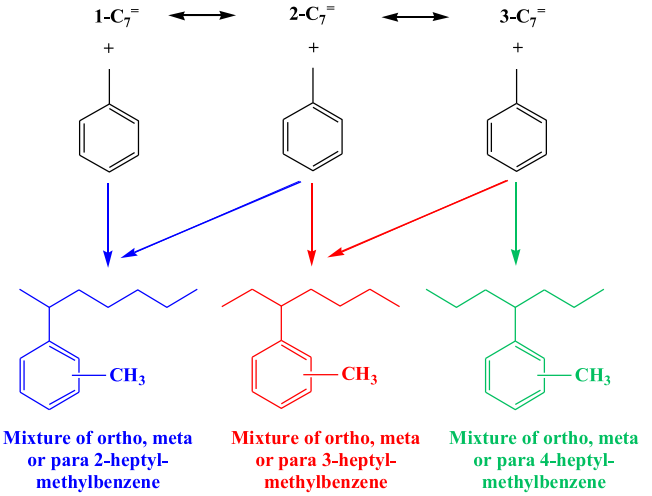

Fig. 1. Formation steps of mono-heptyl-methylbenzene [Magnoux et al., 1997].

hept-1-ene over the surface of different types of zeolite catalysts, as demonstrated in Fig. 1 [Guisnet, 2002].

It should be noted that it is possible to obtain 2- and 3-heptene from double bound shifts of hept-1-ene on the surface of the catalyst. Among the three isomers of heptylmethylbenzene, 2-heptylmethylbenzene is the preferred product because it has a higher biodegradability compared to the other two isomers [S.H. Al-Sultani et al., 2024]. It can be predicted that the coke accumulated during reactions within the catalyst framework is generated from all the formed liquid by products, di- and oligo-merisation of heptene, bi-heptylmethylbenzene, and di-alkylation [Al-Shathr et al., 2023]. Coke selectivity is usually calculated by subtracting the sum of isomerisation and alkylation products from the total percentage.

The aim of this research was study of both experimental and kinetic spectra of complex alkylation reactions of toluene with hept-1-ene. The percentage of conversion and/or concentration selectivity of the products in isomerisation and alkylation reactions, as well as the amounts of coke accumulated on the surfaces of fresh, dealuminated, and desilicated H-beta zeolite catalysts, were compared. The effect of modifying the catalyst framework structure on improving its catalytic behaviour throughout the reaction was investigated, and the different reaction conditions and their impact on the reaction products were also compared and optimized. In fact, mono-heptyl-methylbenzene is a highly sought-after material in industry due to its scarcity and difficulty in obtaining it during this type of alkylation reaction. The study focused on improving the catalytic activity of silicon-rich catalysts to control the slow, specific step of the reaction on their surface. This was achieved by controlling the quantity and distribution of acidic sites within the catalyst structure. This contributed to increasing the reaction selectivity toward this intermediate compound. In other words, it increased the yield of mono-heptyl-methylbenzene on the catalyst surface by reducing the amount of coke accumulated during the reaction.

The main part of this study was related to the use of mathematical modelling to predict the kinetic parameters by applying a sophisticated program that combines nonlinear optimization (genetic algorithm technique) and numerical integration (4th order Runge-Kutta) to accurately calculate and compare the apparent activation energy values for each of the isomerisation and alkylation reactions as well as coke formation. The success of the mathematical model used was confirmed by the compatibility of experimental and theoretical data, as calculations of the apparent activation energies on the surfaces of all catalysts under various reaction conditions used logically matched the results of the experimental reaction conversion.

2. Experimental work

2.1. Catalyst modification

Acid leaching of H-beta zeolite (Alfa Aesar; SiO_2:Al_2O_3 ratio is 360:1) was performed by dispersing 1 g of solid catalyst in 30 mL of 10 M HCl (Sigma-Aldrich; 37 %) using a 50 mL flask under reflux conditions. The mixture heated to 50 °C for 30 min with continuous mixing. When the required time is reached, transfer the flask to ice water immediately to stop the reaction. The solution was separated from the solid using a Heraeus Multifuge 3SR rotary centrifuge. Next, the precipitated solid catalyst was washed several times with distilled water until the pH of the liquid over the zeolite became neutral. The zeolite was then dried at 120 °C for 12 h.

Base leaching began with dispersing 3 g of zeolite in an aqueous solution consisting of 0.1 g NaOH (Sigma-Aldrich; ≥97 %) in 100 mL (i.e., 0.025 M), mixing was performed in a flask combined with reflux. The mixture was heated to 85 °C for 60 min. After reaching the desired time, the flask was instantaneously immersed in ice water to stop the reaction. The same rotary centrifuge was used to separate the zeolite from the aqueous solution and the sediment zeolite was washed several times until the pH reached 7 and then dried at 120 °C for 12 h. The solid zeolite obtained from this treatment was in the Na-form, therefore, it was exchanged to the H-form (i.e., the active acidic form of zeolite) *via* an ion exchange method and using a flask attached to reflux through an aqueous solution of NH_4NO_3 (Acros Organics; ≥99 %) (0.5 M) at 80 °C for 120 min., then calcinated at 450 °C for 240 min to drive out ammonia from the zeolite structure.

2.2. Catalytic reaction system

Laboratory experiments were performed by inserting 10 ml of the feed mixture consisting of toluene (Sigma-Aldrich; ≥99.5 %) and hept-1-ene (Acros Organics; ≥98 %) into a 45 ml stainless steel autoclave, as shown in the Fig. 2, under different operating conditions. Operating conditions included temperature, catalyst weight, toluene: hept-1-ene ratio, and reaction time. Before performing the reaction, all zeolite catalyst samples were activated to remove physiosorbed water and remaining impurities by heating at 150 °C for 2 h. The reaction temperatures used included the ranges 70, 80 and 90 °C at atmospheric pressure with three different weights of zeolite catalyst, namely 0.1, 0.2 and 0.3 g; While the ratios of toluene:hept-1-ene were 1:1, 2:1 and 3:1 under a reaction time of two hours and a stirring speed of 300 rpm. When the reaction time reaches the end, the reactor is placed directly into ice water to stop the reaction. Filter paper was used under vacuum conditions to separate the spent solid catalyst from the liquid reaction products.

Proton magnetic resonance (^{1}H NMR) spectra were recorded on a Bruker AV-400 spectrometer (i.e., ^{1}H: 400 MHz) at room temperature using deuterated chloroform ($CDCl_3$) with tetramethylsilane (TMS) as an internal compound, and a gas chromatography mass spectrometer (GC–MS) from Shimadzu, GCMS-QP2010 SE with DB-1MS column was utilized for qualitative analysis. While quantitative analysis was performed using a Thermo Scientific gas chromatography-flame ionization (GC-FID) TRACE 1310 with a DB-5HT column.

2.3. Modelling and kinetic parameters

2.3.1. Kinetic parameter estimation

Mathematical modelling of chemical reactions can be used to estimate the optimal operating conditions needed to maximize the conversion of reactants and yield toward the desired products [Shakor et al., 2021, Al-Iessa and al., 2023]. The rigorous mathematical model of chemical reactors involves solving the simultaneous differential equations for the transfer of heat, mass and momentum, as well as the kinetic model [Shakor et al., 2020, Shakor et al., 2022]. The kinetic model is the core model used to simulate chemical reactors, in which it describes the distribution of reactants and products within the reaction mixture. Power law, Eley-Rideal (ER) and Langmuir-Hinshelwood-Hougen-Watson (LHHW) models are commonly used in kinetic modelling. In general, the accuracy of a kinetic model increases with the number of kinetic parameters (i.e., activation energy and pre-exponential factors) employed to describe the model. While the linear regression method cannot be used to estimate kinetic parameters for multi-reaction systems, the nonlinear regression method is a powerful technique that can be used in these cases. Non-linear can be performed using one of stochastic optimization methods (i.e.: simulated annealing (SA), harmony search (HS), particle swarm optimization (PSO) and Genetic Algorithms (GA)). In fact, the Genetic Algorithms (GA) are widely utilized for nonlinear optimization and curve fitting of reaction kinetic data with mathematical models [Al-Shathr et al., 2021, Al-Zaidi et al., 2023, Alsaadi et al., 2024, Alsaadi et al., 2025]. The kinetic model deals with toluene alkylation and positional isomerisation on the H-beta zeolite catalyst has not been investigated in previous works. Indeed, most previous studies suffered from some drawbacks in some aspects. For example; some authors neglected the effect of isomerisation and coking reactions in their calculations, such as: Yadav and Doshi [Yadav and Doshi, 2002], Tsai et al. [Tsai et al., 2003] and de Almeida et al. [de Almeida et al., 1994], who

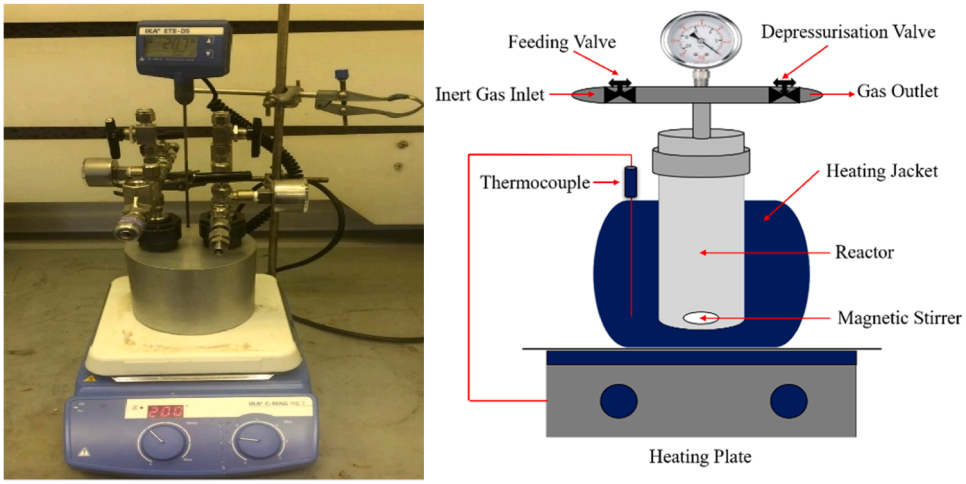

Fig. 2. Image and schematic of the experimental batch reactor.

studied the benzene alkylation with dode-1-cene over non-zeolitic, mordenite and Y catalysts, respectively. Besides, Corma and co-worker [Corma et al., 2000] and Craciun et al. [Craciun et al., 2012] investigated the kinetic of benzene alkylation with propene over Y zeolite and oct-1-ene over MCM-22 zeolite, respectively. Other studies did not take into account the effect of coke such as Aslam et al. [Aslam et al., 2015] during alkylation of benzene with dode-1-cene using mordenite zeolite catalyst. An integrated kinetic model was used in this study. The model has also been simplified using some reasonable assumptions:

1) Concentration and temperature are uniform within the reaction mixture [Perez-Sena et al., 2021], 2) First-order reaction rate [Contrera et al., 2014], 3) Neglecting gaseous products [Feng et al., 2017], and 4) Reaction pressure is one atmosphere [Visan et al., 2019].

However, an equation for mass balance conservation should be developed for each individual component and is as follows.

$$\frac{dC_i}{dt} = \frac{W_c}{V}\sum_{j}^{N_R} a_{i,j} r_j \tag{1}$$

Accordingly, two statistical criteria were used to evaluate the effectiveness of the kinetic model developed in this study, which are mean relative error (MRE) and mean absolute error (MAE). MAE and MRE were calculated using Equations 2 and 3, respectively.

$$\mathrm{MAE} = \frac{1}{N \times M}\sum_{k=1}^{M}\sum_{i=1}^{N}\left|y_{i,k}^{exp} - y_{i,k}^{pred}\right| \tag{2}$$

$$\mathrm{MRE} = \frac{1}{N \times M}\sum_{k=1}^{M}\sum_{i=1}^{N}\left(\frac{y_{i,k}^{exp} - y_{i,k}^{pred}}{y_{i,k}^{exp}}\right) \tag{3}$$

The percentage conversion and percentage selectivity were also calculated using Equations 4 and 5, respectively.

$$\%\ \mathrm{Conversion} = 100\ \mathrm{x}\left[\frac{\text{number of moles of hep} - 1 - \text{tene consumed}}{\text{number of moles of hep} - 1 - \text{tene introduced}}\right. \tag{4}$$

$$\%\ \mathrm{Selectivity} = 100\ \mathrm{x}\left[\frac{\text{number of moles of mono} - \text{heptyl} - \text{methylbenzene}}{\text{number of moles of hep} - 1 - \text{tene consumed}}\right. \tag{5}$$

2.3.2. Kinetic parameters prediction by genetic algorithm

Genetic Algorithm (GA) is a stochastic technique that mimics natural evolution in solving optimization problems, first devised by John Holland in the 1975 [Holland, 1975, Abood et al., 2024, Deshmukh et al., 2024]. GA has been widely studied, tried and applied in many fields in the engineering worlds. The first step in GA is to generate a set of random solutions called the initial population of Npop in the feasible region. GA works on this population and combines (crossover) and modifies (mutates) some chromosomes according to specific genetic operations, towards create a new population with better characteristics. Individuals are selected for reproduction based on their objective functional values and the Darwinian principle of survival of the fittest. The algorithm of the stochastic optimization method of GA is shown in Fig. 3.

3. Results and discussions

3.1. Catalyst characterisation

3.1.1. X-ray diffraction analysis

In the present work, a STOE STADI P type X-ray diffraction operating at a tube voltage and a current of 40 kV and 35 mA, respectively with CuKα1 type radiation and wavelength α = 1.5406 Å was used to analyse zeolite powder samples, the scanning speed was 10° min^{-1} and the running time was 28 min with a 2θ range of 10 to 60° As shown in Fig. 4, increased peak intensity is observed in the dealuminated H-beta zeolite patterns. However, these peaks decrease in the desilicated H-beta zeolite patterns while maintaining acceptable crystallinity. These results are consistent with what was shown by [Li et al., 2009]. In addition, the effect of zeolite modification appeared clearly on the diffraction peaks in the XRD patterns where the 2θ was shifted either to the right-hand side due to dealumination treatment or to the left-hand side owing to desilication treatment. These results are similar to those obtained previously by Al-Zaidi and his co-workers [Al-Zaidi et al., 2012].

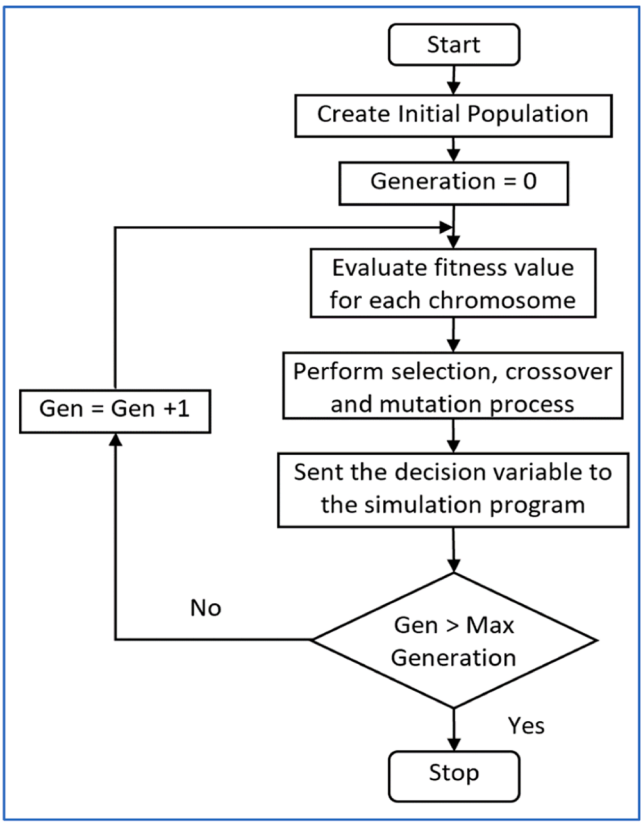

Fig. 3. A diagram of the steps of a genetic algorithm.

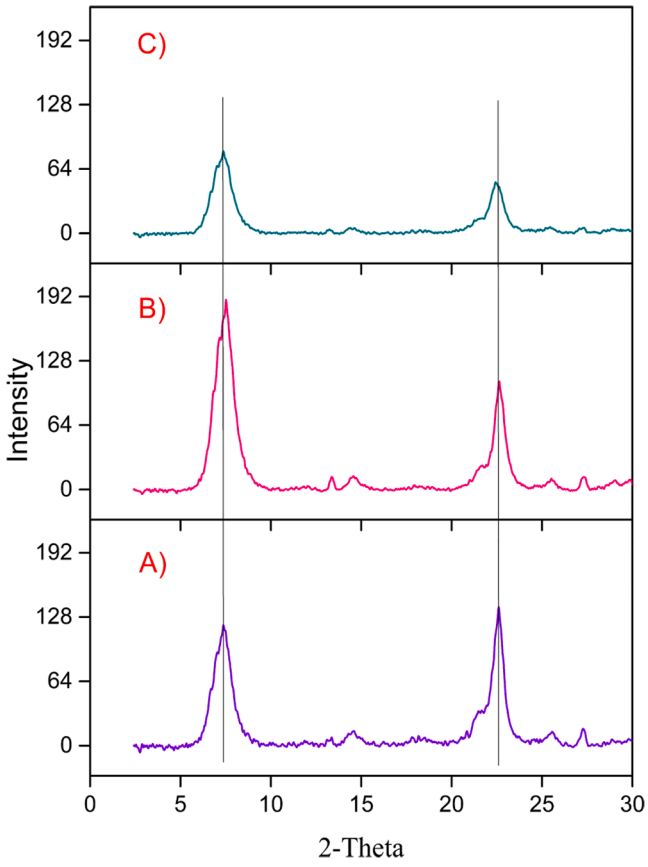

Fig. 4. XRD patterns of (A) fresh, (B) dealuminated, and (C) desilicated H-beta zeolites.

For the purpose of accuracy in calculating the percentage degree of crystallinity resulting from the treatment of the zeolite structure, Eq. (6) was used as follows [Krisnandi et al., 2019]:

$$\%\ Degree\ of\ crystalinity = \frac{\sum\ Relative\ peak\ intensities\ of\ zeolite\ \text{sample}}{\sum Relative\ peak\ intensities\ of\ reference\ sample} \times 100 \quad (6)$$

Table 1 shows the degree of crystallinity of fresh and treated H-beta zeolite samples. Interestingly, the degree of crystallinity of the dealuminated H-beta sample increased to approximately 111 % because the aluminium atoms removed from the structural framework of zeolite led to unit cell shrinkage, as observed from the 2θ range results in the table, a result identical to that obtained in a previous study conducted by Lutz et al., [Lutz et al., 2000]. On the contrary, it decreased after the desilicated treatment to about 49 %. This may have caused partial collapse resulting from the removal of silicon from the structural framework, which naturally leads to the expansion of the unit cell of the treated zeolite. This result is fully consistent with the findings of Bolshakov et al., [Bolshakov et al., 2020] and Silva et al., [Silva et al., 2019].

3.1.2. *Fourier transform infrared spectroscopy (FTIR) analysis*

Shimadzu IRAffinity-1S Fourier transform infrared (FTIR) spectroscopy with a DLATGS detector was used at room temperature for the purpose of evaluating the position of chemical bonds and extent to which these active groups are affected by modifications made to the structure of the zeolite samples. To conduct the FTIR analysis in the range of 400 to 4000 cm^{-1} wavelength. Fig. 5 shows the FTIR spectra of fresh and modified H-beta zeolite samples. In fact, the IR spectra of the modified zeolites almost match the functional groups of the untreated parent zeolite and agree with the shifting results observed for the unit cell in the XRD patterns of the treated samples. Furthermore, the vibrational spectroscopy is similar to what has been demonstrated in previous studies by [Klunk et al., 2020, Wei et al., 2019, J. Li et al., 2017].

A band in the region of 410–450 cm^{-1} is attributed to the asymmetric stretching of Al-O and Si-O [Narayanan et al., 2015]. Wavelengths between 525–570 cm^{-1} are assigned to the stretching vibrations of the SiO_4 tetrahedron [Mintova et al., 2006], while the bands at 570–650 cm^{-1} are related to the exterior peak of the double ring connected to the zeolite structure [Saleh et al., 2018]. The bands between 690–805 cm^{-1} represented the symmetric stretching vibration of either O-Si-O or O-Al-O [Azzolina Jury et al., 2013]. Wavelengths around 900–950 cm^{-1} corresponded to the linkage of Si-O groups on the outer surfaces of crystals [Wei et al., 2019]. It was observed that these bound disappeared as a result of the reaction of NaOH with the silanol groups during the desilication modification, and the same result was earlier obtained by Chalupka et al., [Chalupka et al., 2018]. The transmittance bands at 1050–1070 cm^{-1} are associated with symmetric Si-O-Si or Al-O-Al [Azzolina Jury et al., 2013]. Obviously, these bands after

Table 1
Degree of crystallinity according to XRD results fresh, dealuminated and desilicated H-beta zeolite samples.

Fresh H-beta		Dealuminated H-beta		Desilicated H-beta	
2θ	Intensity	2θ	Intensity	2θ	Intensity
7.37	119.848	7.55	185.237	7.34	79.656
13.31	5.655	13.37	12.537	13.16	2.776
14.51	13.883	14.6	12.735	14.42	5.308
21.44	32.14	21.68	23.884	21.41	13.353
22.58	136.044	22.61	107.055	22.46	50.056
Total	∑307.57	Total	∑341.448	Total	∑151.149
Degree of crystallinity percentage using fresh H-beta as a reference					
	100 %		111 %		49.1 %

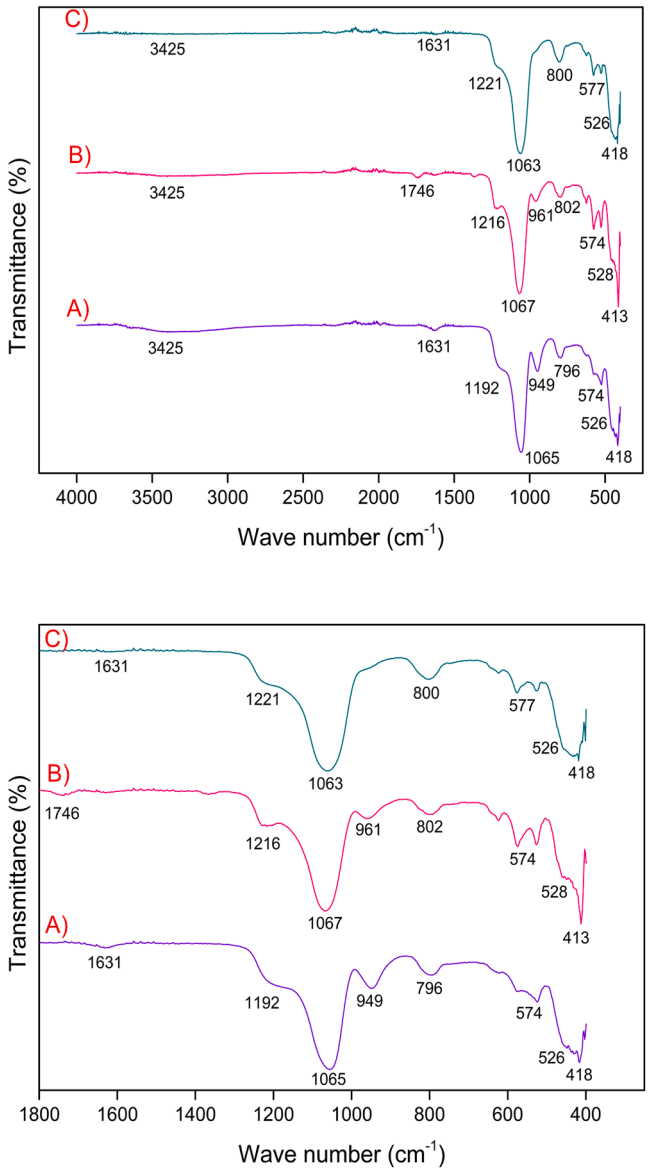

Fig. 5. FTIR spectra of (A) fresh, (B) dealuminated, and (C) desilicated H-beta zeolites.

dealumination treatment shifted to higher wave numbers due to the diminish in aluminium content, and the same conclusion was achieved by Sohn and his co-workers [Sohn et al., 1986]. In addition, the bonds at 1190–1230 cm^{-1} and 1620–1750 cm^{-1} indicate the -OH vibration according to [Klunk et al., 2020], whereas the wavelength at around 3200–3500 cm^{-1} represents the stretching vibrations for Si-OH based on [Narayanan et al., 2015]. On the other hand, for the desilicated H-beta, it is observed that the Si-OH bond disappears compared to the parent H-beta sample as a result of the silanol nests generated due to this treatment [Silaghi et al., 2014]. The same situation appeared in the IR spectra of the dealuminated H-beta sample, which is attributed to the removal of aluminium species and the configuration of a silanol nest around the defect sites formed during this treatment [Adriano et al., 2022].

3.1.3. Scanning electron microscope (SEM) analysis

A JEOL JSM-6010LA scanning electron microscopy (SEM) instrument was used to capture SEM images to analyse the surface morphology of the zeolite specimens. It should be noted that this analysis involves coating the surface of the sample with gold for 10 s with an argon atmosphere using AGAR SPUTTER COATER, B7340 under a voltage of 15 kV at a fixed magnification of 500 times (50 μm). Fig. 6 shows that all samples have a rough quasi-spherical surface morphology. It is clear that both parent and modified samples have an almost uniform topography, in other words, no significant effect appears on the surface morphology after acid or alkaline treatment. These observations are consistent with those previously made by Altındaş et al., [Altındaş et al., 2023] and Quintana-Gómez et al., [Quintana-Gómez et al., 2022]. In addition, it is natural that after modifications the structure of zeolite and removing the Si or Al atoms from its lattice, the edges of zeolite particles tend to be more blurry and irregular, with the observation of some division within the large particles become smaller, especially after being exposed to desilication treatment using caustic soda, and this may be due to a partial collapse in the crystalline structure of zeolite, as indicated by the XRD patterns. A similar conclusion was obtained by Wang et al., [Wang et al., 2016].

3.1.4. Nitrogen adsorption analysis

A Micromeritics instrument was utilized to measure the surface area and pore volume of zeolite samples according to the Brunauer, Emmett, and Teller (BET) method and based on the phenomenon of N_2 gas adsorption-desorption isotherm, with the data analysed using 3Flex software version 3.02. Fig. 7 shows all sorption isotherms of fresh, dealuminated and desilicated H-beta zeolites. The shape of the adsorption or desorption branch may be mechanistically attributed to the pore structure of a solid. Such that the analysis of the adsorption-desorption hysteresis loop is essential to get a complete picture about the main structure of the pores within the sample. The formation of framework mesopores, less of micropores, within the structure normally gives rise to adsorption-desorption hysteresis loops. Generally, a total pore volume of solid "adsorbent surface" can easily be found, if the density of gas "adsorbate" is known. It is clear that the fresh and dealuminated samples demonstrate an IUPAC-type I hysteresis loop curve according to BDDT-classification indicating the presence of micropores. However, the desilicated sample typically showed type IV denoting the existence of both micropores and mesopores. Similar results were obtained by Zhang et al., [Zhang and al., 2018] and Li et al., [Q. Li et al., 2017].

It is also noted in Table 2 that the surface area decreased after the dealuminated treatment to become 411 $m^2/g_{cat.}$. On the contrary, an increase in the surface area was observed after desilication modification, reaching 647 $m^2/g_{cat.}$ when compared to the BET-area of the parent sample. The same behaviour was repeated with the total pore volume, where the value of the total pore volume decreased as a result of the dealuminated modification and in return increased after the desilication modification. Wang et al., [Wang et al., 2016] and Al-Zaidi et al., [Al-Zaidi et al., 2012] demonstrated the same behaviours for zeolite textural parameters in their studies.

3.1.5. Inductively coupled plasma analysis

A Fisons Horizon ICP-AES instrument with argon plasma was used to measure the Si/Al ratio by estimating the metal contents of fresh and treated beta-zeolite specimens. The dealuminated sample showed an increase in the Si/Al ratio, reaching 563 compared to the parent sample that had Si/Al of about 367. In contrast, the effect of desilication treatment was evident on the Si/Al ratio as it decreased to 231 compared to the fresh sample. These results were identical to those obtained by Li and his co-worker [Li et al., 2023]. It should be noted that an increase in the Si/Al ratio of the catalyst sample indicates a decrease in its acidity. Conversely, a decrease in the Si/Al ratio reveals the high acidity of the zeolite catalyst sample.

Table 3

3.1.6. Thermogravimetric (TGA) analysis

Thermogravimetric analysis (TGA) was performed to measure the percentage of coke formed during the alkylation of toluene with hept-1-ene using a PerkinElmer TGA 4000 analyser and approximately 15 mg of

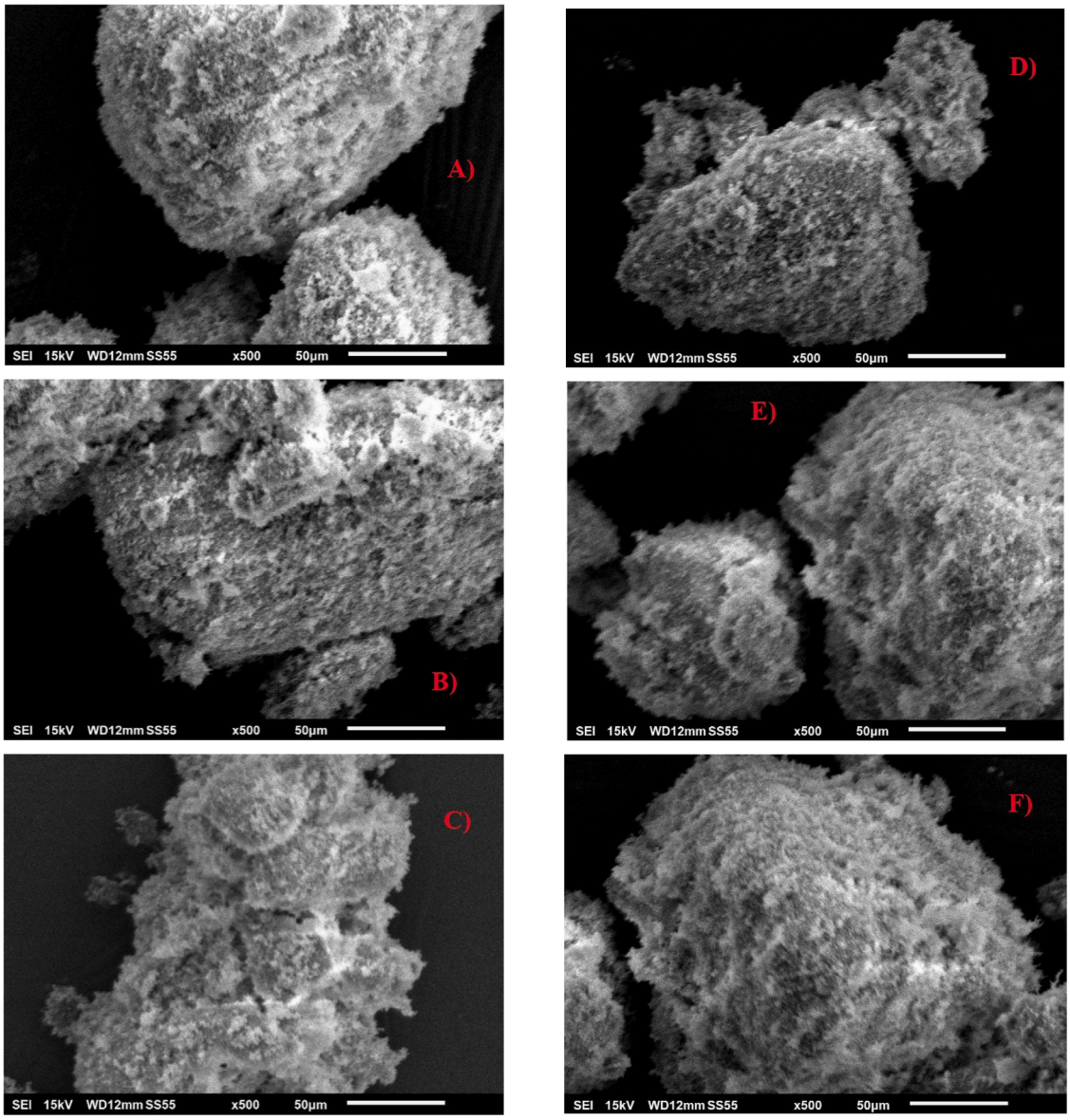

Fig. 6. SEM images of (A) & (B) fresh, (C) & (D) dealuminated and (E) & (F) desilicated H-beta zeolites.

sample each time. The pyrolysis temperature was varied from room temperature to 800 °C at a heating rate of 10 °C min^{-1}. Initially, nitrogen gas was used at a flow rate of 20 mL/min to drive out physically absorbed water and unwanted volatiles, then air was used instead of inert gas at the same flow rate to burn off the accumulated coke and consequently calculate the total amount of coke. The coke percentage was calculated according to Eq. (7):

$$coke\% = \frac{Weight\ of\ sample\ at\ 200\ ^{\circ}C - Weight\ of\ sample\ at\ 800\ ^{\circ}C}{Weight\ of\ sample\ at\ 800\ ^{\circ}C} \times 100 \quad (7)$$

Fig. 7 shows the TGA curves of post-reaction spent catalysts, including fresh, dealuminated, desilicated H-beta zeolite at different reaction temperatures of 70, 80, and 90 °C. In general, the weight loss prior to 200 °C represents volatiles which are partially linked to the structural framework of the catalyst *via* Van der Waals forces. While the TG curves after 200 °C were divided into two basic steps of weight loss from the used-up catalyst. The first step occurs between 200–400 °C and represents the decomposition of soft coke, and the second decomposition step takes place between 400–800 °C and represents the percentage of hard coke build-up. These results are consistent with what was previously found by other researchers, such as [Wang and Manos, 2007].

Fig. 8

The amount of coke was determined from the TG curves. Fig. 9 illustrates the effect of zeolite modification on the total percentage of coke accumulation during toluene alkylation with hept-1-ene at different reaction temperatures. It can be seen that the amount of coke decreased after the dealumination and desilication modifications compared to the amount accumulated on the parent sample. Simultaneously, the effect of the reaction temperature is very clear, as it was found that the percentage of coke precipitated on the surface of the catalyst decreases with the increase in the reaction temperature because the raise in temperature leads to an acceleration of this type of reaction and thus an increase in the yield as the deposited coke decreases. Other researchers have reached the same conclusions, such as Wang and co-worker [Wang et al., 2016] and Silaghi et al., [Silaghi et al., 2014]. In addition, Moljord [Moljord et al., 1995] studied this type of reaction and stated the following: "The total coke content decreases slightly with increasing reaction temperature due to the slightly greater temperature dependence of coke precursors compared with hard coke. Because it is a reaction-activated process, transformation of coke precursors into hard

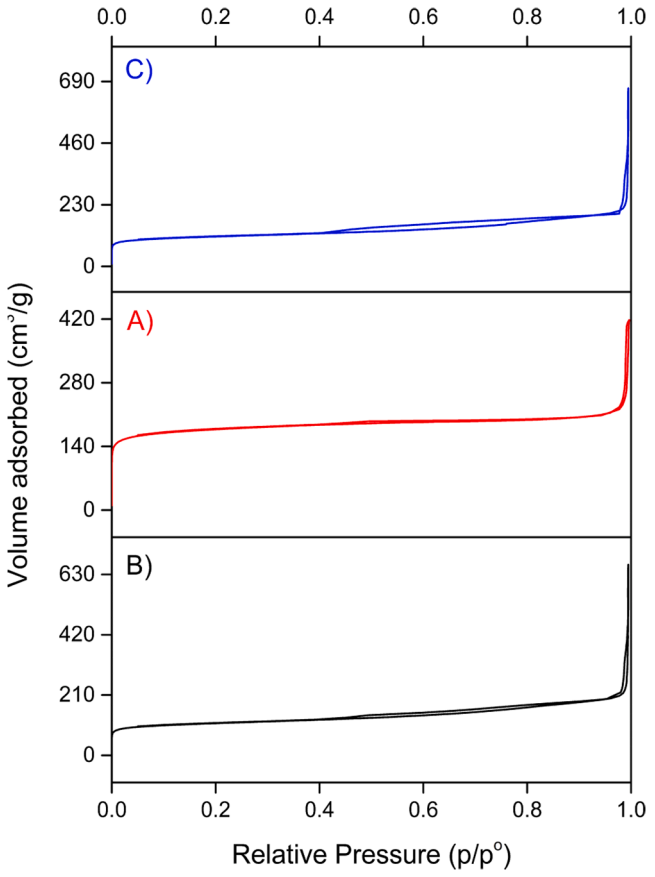

Fig. 7. BET-profile of (A) fresh, (B) dealuminated and (C) desilicated H-beta zeolites.

Table 2
BET- surface area and pore volume of fresh, dealuminated and desilicated H-beta zeolites.

Zeolite sample	S_{BET} (m^2/g)	V_{tot} (cm^3/g)	V_{mic} (cm^3/g)	V_{meso} (cm^3/g)
Fresh H-beta	598	0.334	0.214	0.120
Dealuminated H-beta	411	0.311	0.206	0.105
Desilicated H-beta	647	0.349	0.121	0.228

Table 3
ICP-Si/Al mole ratio of fresh, dealuminated and desilicated H-beta zeolites.

Zeolite sample	ICP-Si/Al
Fresh H-beta	367
Dealuminated H-beta	563
Desilicated H-beta	231

coke is likely faster at high reaction temperature".

3.2. Liquid NMR analysis

Chemical shifts (δ) are determined in parts per million with solvent resonance (i.e. $CHCl_3$: δ 7.20 ppm). Data collected from ^{1}H NMR were assigned based on the partitioning patterns, which were identified as 's' for single, 'd' for double, 't' for triple, 'q' for quadruple, and 'm' for multiple. The ^{1}H NMR spectrum of the crude compound indicates the presence of three isomers, namely 2-heptyl-methylbenzene, 3-heptyl-methylbenzene, and 4-heptyl-methylbenzene. However, according to

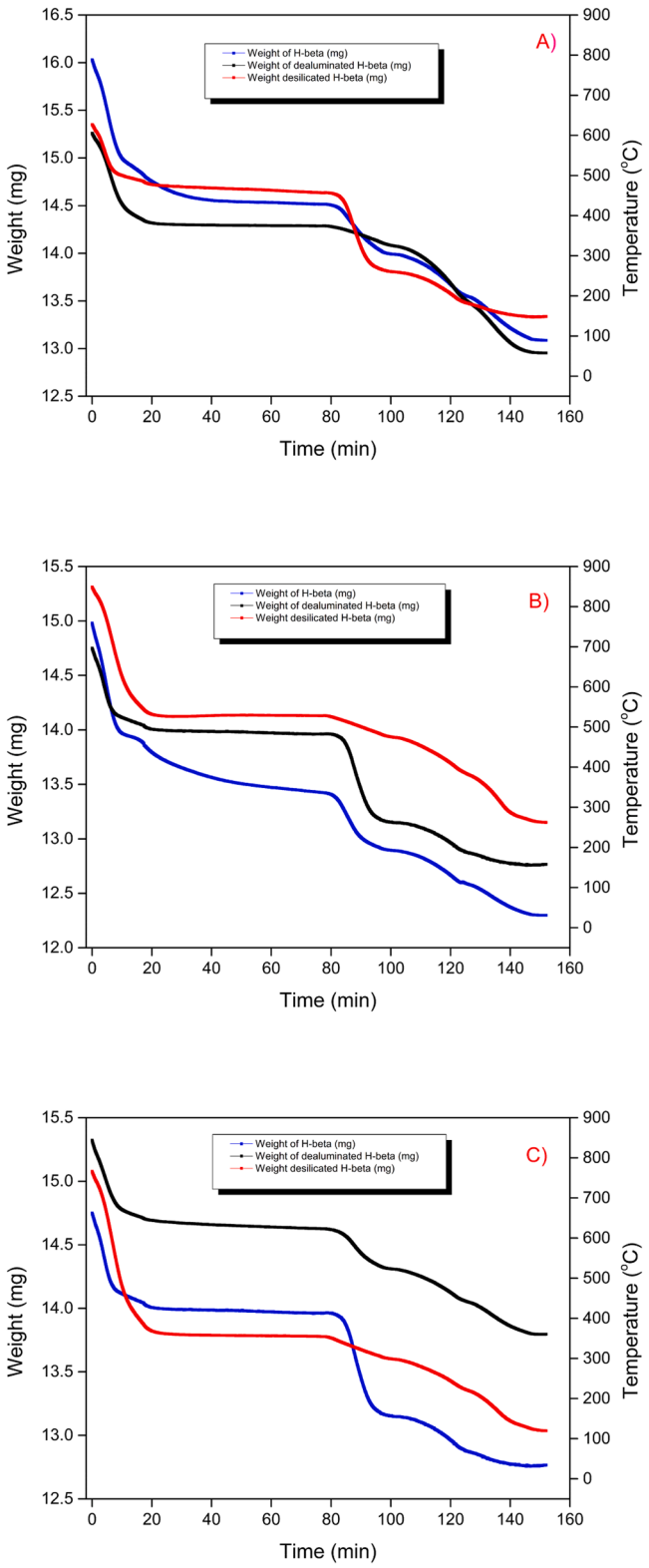

Fig. 8. TGA profiles of spent H-beta zeolite catalysts through toluene alkylation with hept-1-ene at (A) 70 °C, (B) 80 °C and (C) 90 °C for.

the low stability, 1-heptyl-methylbenzene was not detected in the product, as also confirmed by [Yuan et al., 2002].

Thin layer chromatography (TLC) was performed on silica of the crude compound and visualised using an alkaline aqueous solution of potassium permanganate ($KMnO_4$). The crude compound was purified by column chromatography using an eluent of ethyl acetate:petroleum

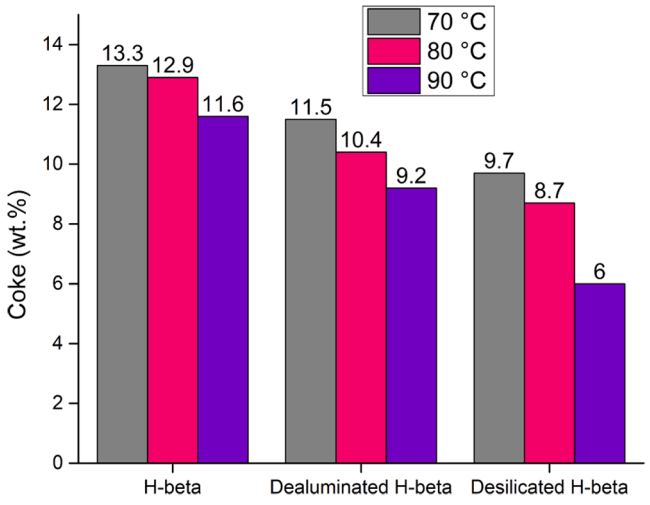

Fig. 9. Coke percentage formed during toluene alkylation with hept-1-ene over parent, dealuminated and desilicated spent H-beta zeolite catalysts.

ether 1:4 with *Rf* = 0.6. In the ^{1}H NMR spectrum in Fig. 10 shows δ_H = 7.05–7.28 (4H, m, ArCH) substituted aromatic carbons, δ_H = 2.60–2.70 (1H, m, CH), δ_H = 2.35 (3H, s, CH_3), δ_H = 1.50–1.70 (2H, m, CH_2), δ_H = 1.15–1.35 (6H, m, CH_2), and δ_H = 0.8 (3H, t, CH_3). The above data confirmed that 2-heptyl-methylbenzene is the main isomer compared to all other spectroscopic measurements, and it is the main product of the isomer formations obtained from the retaining the configurations of the rest of the other isomers. These findings are consistent with the outcomes of a previous study conducted by Pérez-Guevara et al., [Pérez-Guevara et al., 2020] and Aliyeva et al., [Aliyeva et al., 2021].

3.3. Discussion of experimental results

The effect of different operating conditions on the alkylation of toluene with hept-1-ene was studied using fresh and modified H-beta zeolite catalysts. It is worth noting that the type and quantity of isomerisation products depends mainly on several fundamental operational factors, such as reaction time, reaction temperature, aromatic: olefinic ratio, and the amount of catalyst. Fig. 11 shows the effect of reaction time on the concentration of reactants and products. It is clear that the effect of time decreased to less than about 5 % after the first hour of reaction, which means that the three samples of catalysts almost reached stability. Therefore, 60 min was chosen as the preferred reaction time for all upcoming experiments. This finding is consistent with Cadenas and co-workers [Cadenas et al., 2014] who reported that the conversion of 1-hexene reached a maximum within 60 min during a study of toluene alkylation with 1-hexene over Amberlyst 35 and Purolite CT-275.

Fig. 12 illustrates the effect of the amount of H-beta zeolites on the reactions of: a) isomerization, b) alkylation and c) coking formation using catalysts with different Si/Al ratios (i.e., fresh (367), dealuminated (563) and desilicated (231)) under the reaction conditions set at a temperature of 90 °C, the ratio of toluene:Hept-1-ene 3:1 and the reaction time 60 min.

In general, both types of catalyst modification indicate an improvement in the conversion of double-bond isomerisation and alkylation products with a significant reduction in the amount of accumulated coke compared to the fresh sample. It can be seen that increasing the amount of zeolite catalyst contributed to increasing the selectivity of isomerisation and alkylation products, coinciding with a striking decrease in coke selectivity, as catalysis is an interfering phenomenon that depends mainly on the surface available for the reaction. It is observed in Fig. 12 (a-b) that there is an increase in the selectivity of isomerisation and alkylation products by about two times when using 0.3 g of zeolite catalyst compared to 0.1 g of the same catalyst. In addition, comparing the results of the alkylation reaction on the surfaces of fresh and modified zeolite samples using a weight of 0.3 g catalyst showed a significant increase on the surfaces of the modified samples. However, the isomerism selectivity on the surface of the dealuminated sample was relatively high, reaching 55 % compared to the results on the surface of the fresh sample, which amounted to 48 %, while that selectivity increased slightly on the surface of the desilicated sample, reaching only 50 %. This is because the acidity and surface properties of the fresh H-beta catalyst sample is more suitable for the isomerisation reaction rather than the alkylation reaction, as indicated by previous studies [Al-Zaidi et al., 2023, Wang et al., 2023, Lee et al., 2023, Barakov et al., 2022]. Accordingly, increasing the amount of catalyst provided a high surface area that increased contact between the reactants and the catalyst within a shorter reaction time, which in other words led to accelerating the slow step specified for the reaction and avoiding rapid deactivation. These results are consistent with what was concluded by [Faghihian and Mohammadi, 2012]. It is noted in Fig. 12(c) that there is a significant decrease in coke selectivity when using an additional amount of zeolite catalyst, for example, the amount of coke accumulated decreased from 56 % when using 0.1 g of dealuminated catalyst to reach down to about 14 % when the amount of catalyst was increased to 0.3 g. This is due to the increased stability of the catalyst, which acts to increase the resistance of the catalyst to deactivation through reducing carbon deposition, taking into account the increase in the cost of the production process with the increase in the amount of catalyst used

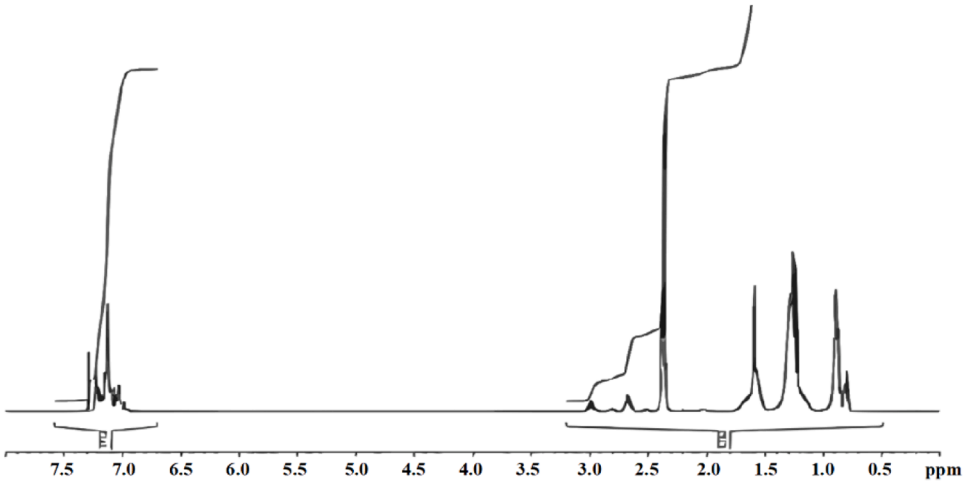

Fig. 10. ^{1}H NMR spectrum of 2-heptyl-methylbenzene.

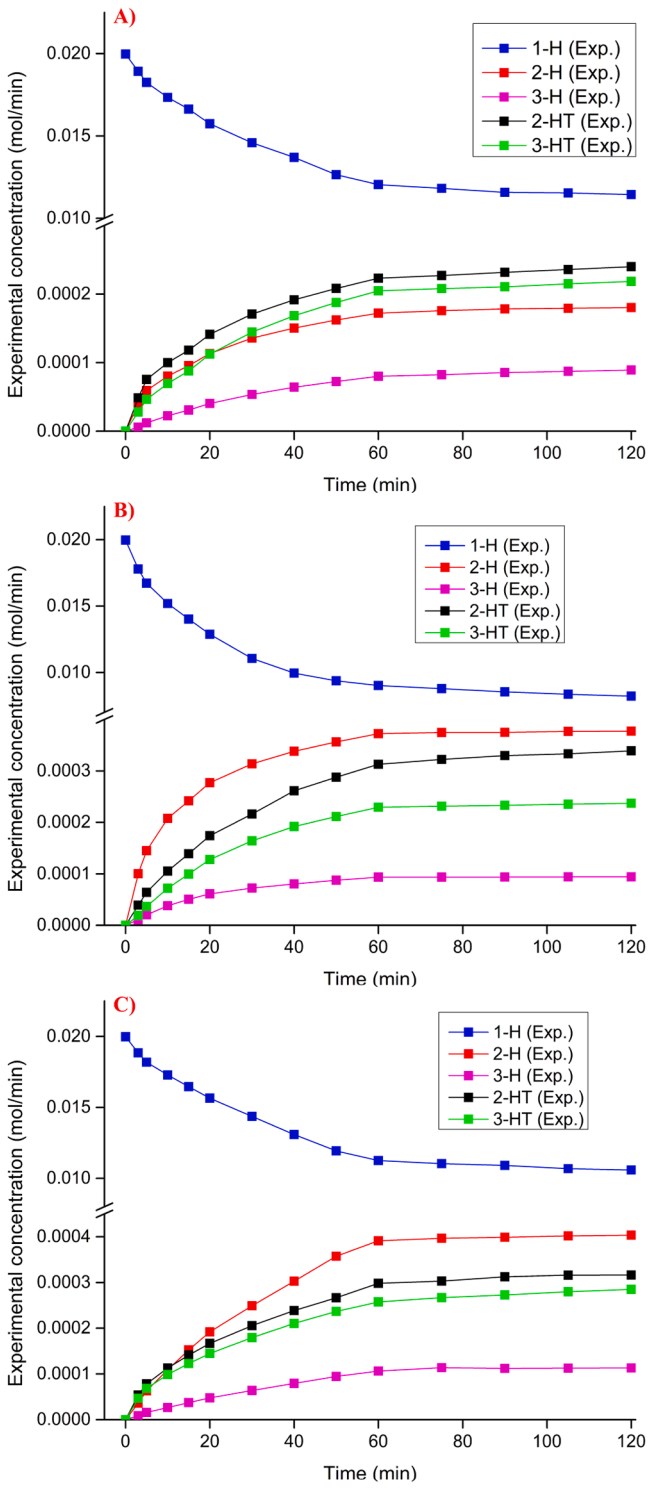

Fig. 11. Concentrations of reactant and products of toluene alkylation with hept-1-ene over H-beta zeolite catalysts: A) fresh, B) dealuminated and C) desilicated at 90 °C, 0.3 g catalyst weight, 3:1 toluene:hept-1-ene ratio and 120 min reaction time.

[Shakor and Shafei, 2023].

The effect of the reaction temperature on the selectivity toward isomerisation and alkylation as well as coke formation was investigated during the alkylation reaction of toluene with hept-1-ene over the surfaces of fresh and modified H-beta catalysts in a temperature range between 70–90 °C, while maintaining all other operating conditions are constant. The main reason for choosing lower reaction temperatures is

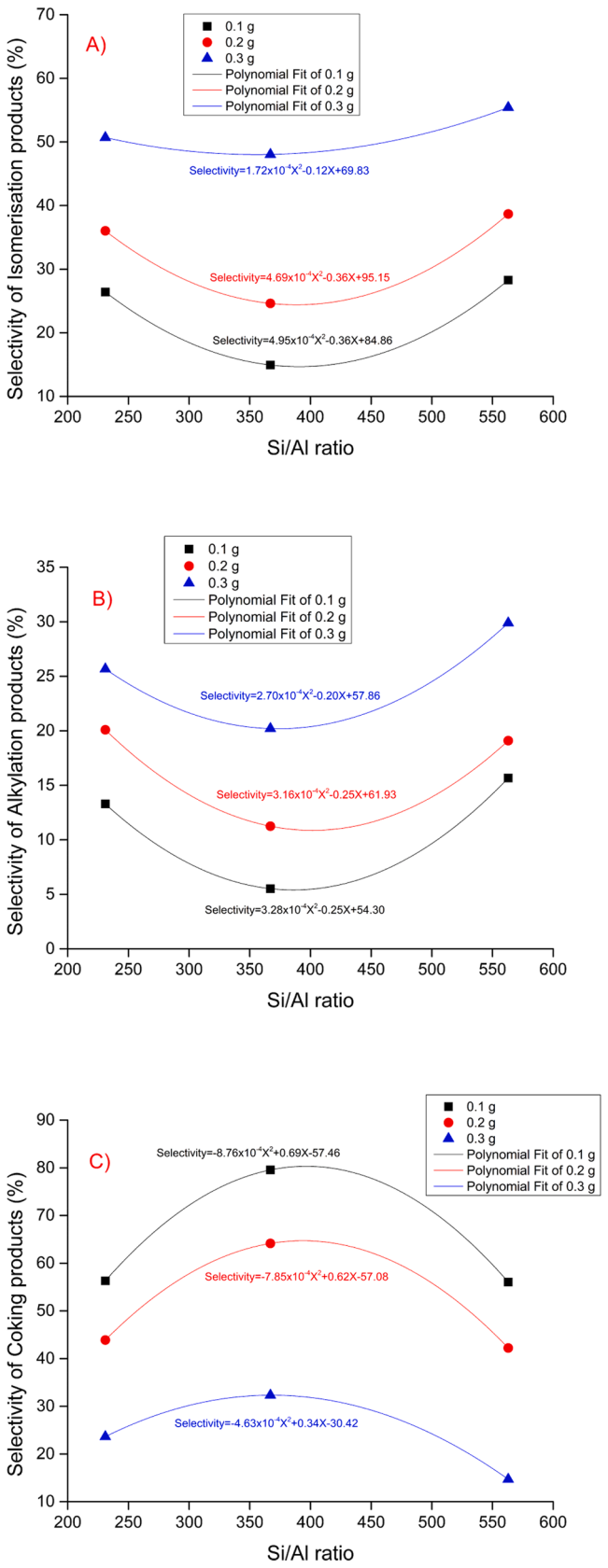

Fig. 12. Selectivity towards A) hept-1-ene isomers, B) mono-heptyl-methylbenzene and C) coke accumulation in the alkylation reaction of toluene with hept-1-ene using different amounts and Si/Al ratios of catalysts.

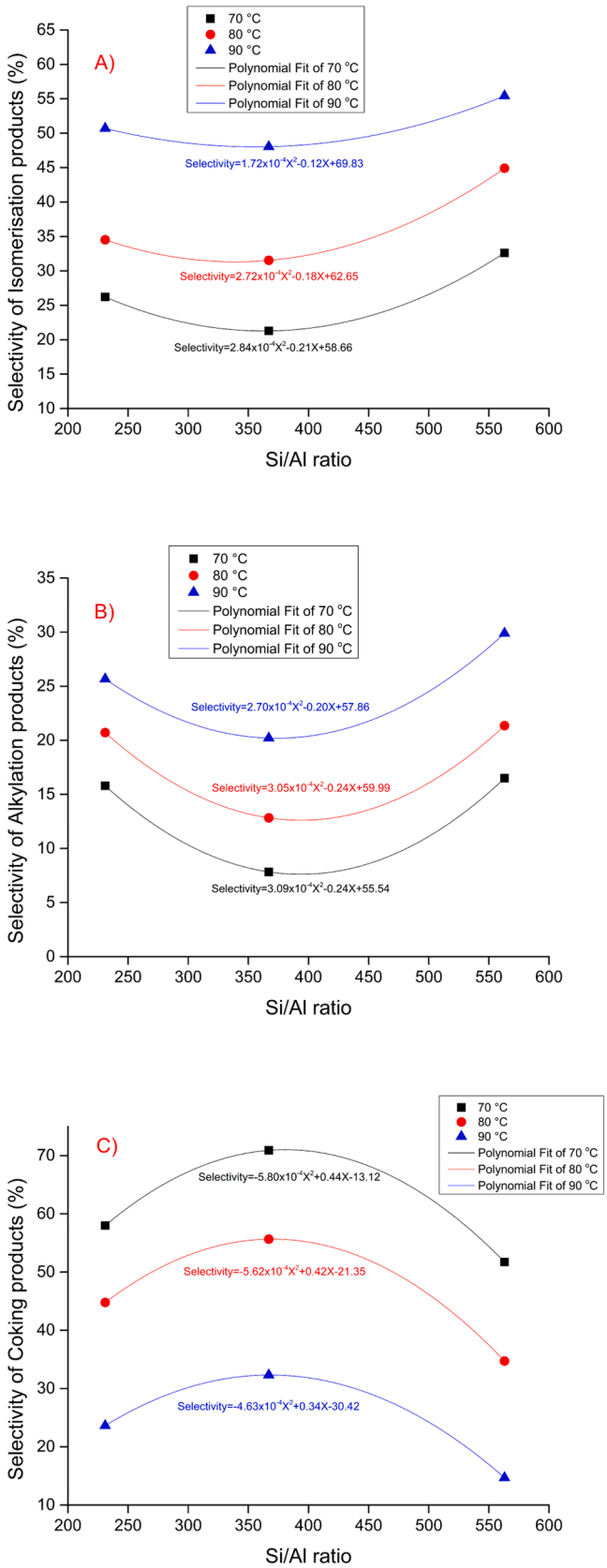

Fig. 13. Selectivity towards A) hept-1-ene isomers, B) mono-heptyl-methylbenzene and C) coke accumulation in the toluene alkylation with hept-1-ene at various reaction temperatures and over the surfaces of catalysts with different Si/Al ratios.

due to the nature of the alkylation reaction as an exothermic reaction [Tsai et al., 2003]. In general, it is observed that selectivity increases towards both alkylation and isomerisation products with increasing reaction temperature while the resulting coke concentration decreases as in Fig. 13, because most of the side reactions have decreased and this is mainly due to the high rate of alkylation and isomerisation as dominant products. These results are consistent with other studies conducted on this type of complex interactions [Cowley et al., 2005]. Dealuminated H-beta zeolite showed a noticeable improvement in selectivity towards isomerisation and alkylation compared to the parent H-beta. This is due to the increase in the Si/Al ratio for this sample, which contributed to reducing the amount of coke accumulated inside the pores of the catalyst as an inevitable result of the diminish in the acidity of the zeolite, which is the main factor responsible for the formation of coke. Moreover the increase in the structural crystallization of the catalyst subsequent to the dealumination treatment, as previously shown from XRD analysis, may have led to an increase in its catalytic activity and thus improved behaviour of the reaction mechanism over the catalyst surface, according to the published literature [K. Zhang et al., 2018]. In the same context, the desilicated sample showed a noticeable progress in selectivity on its surface towards isomerisation and alkylation compared to the parent sample, although it was somewhat less than that found on the surface of the dealuminated sample. This could be a result of the formation of a mesoporous structure and a decrease in the degree of crystallinity of its lattice, as revealed by BET and XRD analyses respectively, which led to an increase in coke generation on its surface owing to the high acidity of the catalyst compared to the dealuminated one. These interpretations are consistent with what other published studies have suggested [Han et al., 2022].

Three different ratios (i.e. 1:1, 2:1 and 3:1) of toluene: hept-1-ene as feedstock were studied for the alkylation reaction of toluene with hept-1-ene on catalysts with different Si/Al ratios, and the results are demonstrated in Fig. 14. In these results, positional isomerisation of hept-1-ene and alkylation of toluene are the main reactions while heptyl-methylbenzenes are the crucial products according to the known reaction mechanism [Cadenas et al., 2014]. In fact, a higher toluene: hept-1-ene ratio contributes to a more economical reactor size because the total conversion of hept-1-ene can reduce side reactions [Cowley et al., 2005].

In other words, the lowest ratio (i.e., 1:1) of the feed contributes to increasing the possibility of side reactions such as: dialkylation of toluene and dimerization of hept-1-ene means increased possibility of faster deactivation of the catalyst [Horňáček et al., 2009]. The results on the surfaces of the modified zeolite samples exhibited a considerable improvement in selectivity towards isomerisation of hept-1-ene and alkylation of toluene with hept-1-ene by using high feedstock ratios. Scientifically, the transalkylation reaction is still an acceptable explanation that describes the impact of high toluene percentage on the selectivity of the isomerism of mono-heptyl-methylbenzene and hept-1-ene, according to the published literature [Guisnet, 2002]. On the other hand, it was observed that the selectivity towards coke formation decreased to its lowest value when using the highest ratio of toluene: hept-1-ene (i.e. 3:1) because toluene works to push the reaction with mono- and di-heptyl-methylbenzene that trapped inside the zeolite pores. Consequently, they are converted into the desired heptyl-methylbenzene products. These results agree with the explanations of other researchers [Da et al., 2001].

3.4. Kinetic model

3.4. 1 kinetic study using fresh, dealuminated and desilicated zeolite catalysts

The main benefits of studying reaction kinetics are summarized in choosing the best operating conditions that give the highest possible yield, as well as choosing the appropriate catalyst that gives the highest catalytic activity and stability during the reaction [Qi et al., 2018,

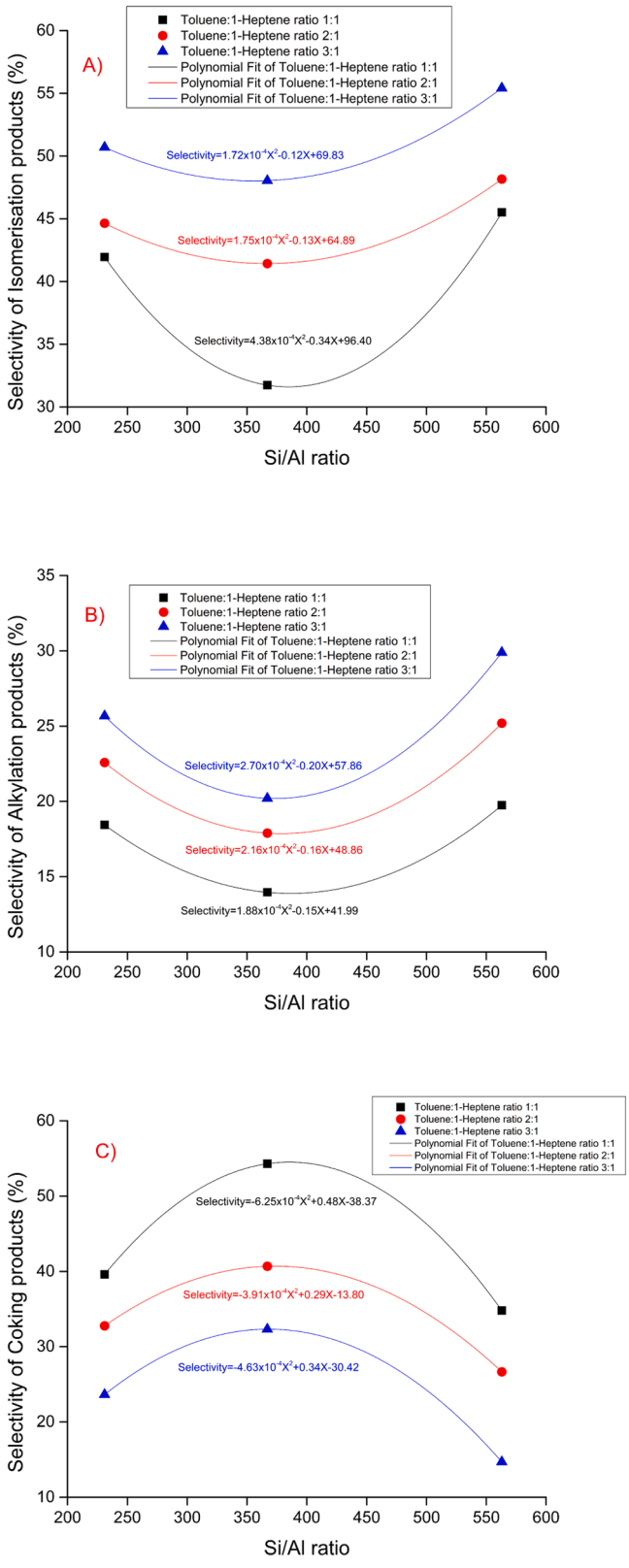

Fig. 14. Selectivity towards A) hept-1-ene isomers, B) mono-heptyl-methylbenzene and C) coke accumulation in the toluene alkylation with hept-1-ene at various toluene:hept-1-ene ratios and over the surfaces of catalysts with different Si/Al ratios.

Struebing et al., 2013]. It is preferable to study the reaction kinetics in a batch reactor because the change in the concentration of the reactants and products being measured occurs instantaneously, as the selectivity of the main products is increased to the highest values, and the reaction temperature can be controlled precisely [Al-Shathr et al., 2022]. The present reaction is evaluated as pseudo-first order kinetics because the toluene concentration throughout the reaction remains approximately constant depending on the high ratio of toluene:hept-1-ene used [Siffert et al., 2000]. Because the kinetic diameter of toluene and the pore size of the catalyst play a crucial role in identifying the appropriate kinetic model, the Eley-Rideal kinetic model is chosen as the most acceptable model [Craciun et al., 2012].

In this model the alkylation of toluene can be simulated with hept-1-ene due to the fitting kinetic diameter of toluene of ~5.85 Å [Jae et al., 2011] compared to the H-beta pore size of ~6.5 Å [Busca, 2014]. In this study, a developed kinetic model was derived based on the proposed elementary reaction steps of the mechanism shown in Fig. 1 previously using power law and mass balance equations for a batch reactor. Since the linear least square approximation method cannot be applied to predict the kinetic parameters of reversible reactions or multiple simultaneous reaction systems, the kinetic model parameters were estimated by solving the differential equations for all chemical species employing the optimization-integration approach according to the results obtained experimentally.

In addition, minimization of the objective function, which is defined as the mean relative error, was achieved using the genetic algorithm optimization method implemented in MATLAB R2021b software. To calculate the model's predicted concentrations of reactants and products, the seven ordinary differential equations (ODEs) were solved simultaneously using the fourth-order Runge-Kutta numerical integration method, taking into account that the kinetic parameters are estimated at all iteration. Reaction rate constants were expressed in the form of the Arrhenius equation to take into consideration the influence of temperature. Therefore, kinetic parameters were obtained for three different catalysts, with six trials for each catalyst.

In fact, these experiments are governed *via* basic parameters, which include the change in temperature, the ratio of toluene to heptane, and the weight of the catalyst. Figs. 15–17 represent the comparison between the theoretically predicted data based on mathematical results and the practical data based on laboratory experiments conducted on parent, dealuminated, and desilicated H-beta catalysts, respectively. The dotted lines in the figures represent the experimental results while the solid lines represent the model predictions. Figs. (15H, 16H, and 17H) demonstrate the parity plot for those three catalysts. The values of the mean relative errors were found to be 10.59, 12.15 and 13.31 % for the parent, dealuminated, and desilicated H-beta catalysts, respectively. It is noteworthy that the level of errors obtained is considered moderate because each catalyst was tested using six experiments under different operating conditions. Automatically, increasing the number of experiments performed or the number of components within the reaction mixture will be also increased the resulting error levels.

It should also be noted that the concentration was measured over time in the batch reactor in this study, while the concentration could not be measured as the weight of the catalyst changes along the length of the fixed bed reactor. This explains why higher levels of error appear when studying the kinetic reaction in batch reactors compared to fixed bed reactors. Hence, batch reactors are more suitable for accurate error checking though studying the kinetic behaviour of a simultaneous multi-reaction system compared to fixed bed reactors.

The estimated activation energy (E) values are shown in Table 4. It can be observed that the activation energy for hept-1-ene isomerisation is lower than the activation energies obtained for the alkylation and coke formation reactions on the surfaces of the three catalysts. In other words, it can be concluded that the speed rate of the isomerisation reactions is faster than the speed rates of the other reactions. In generally, the overall activation energies of the isomerisation reactions were found

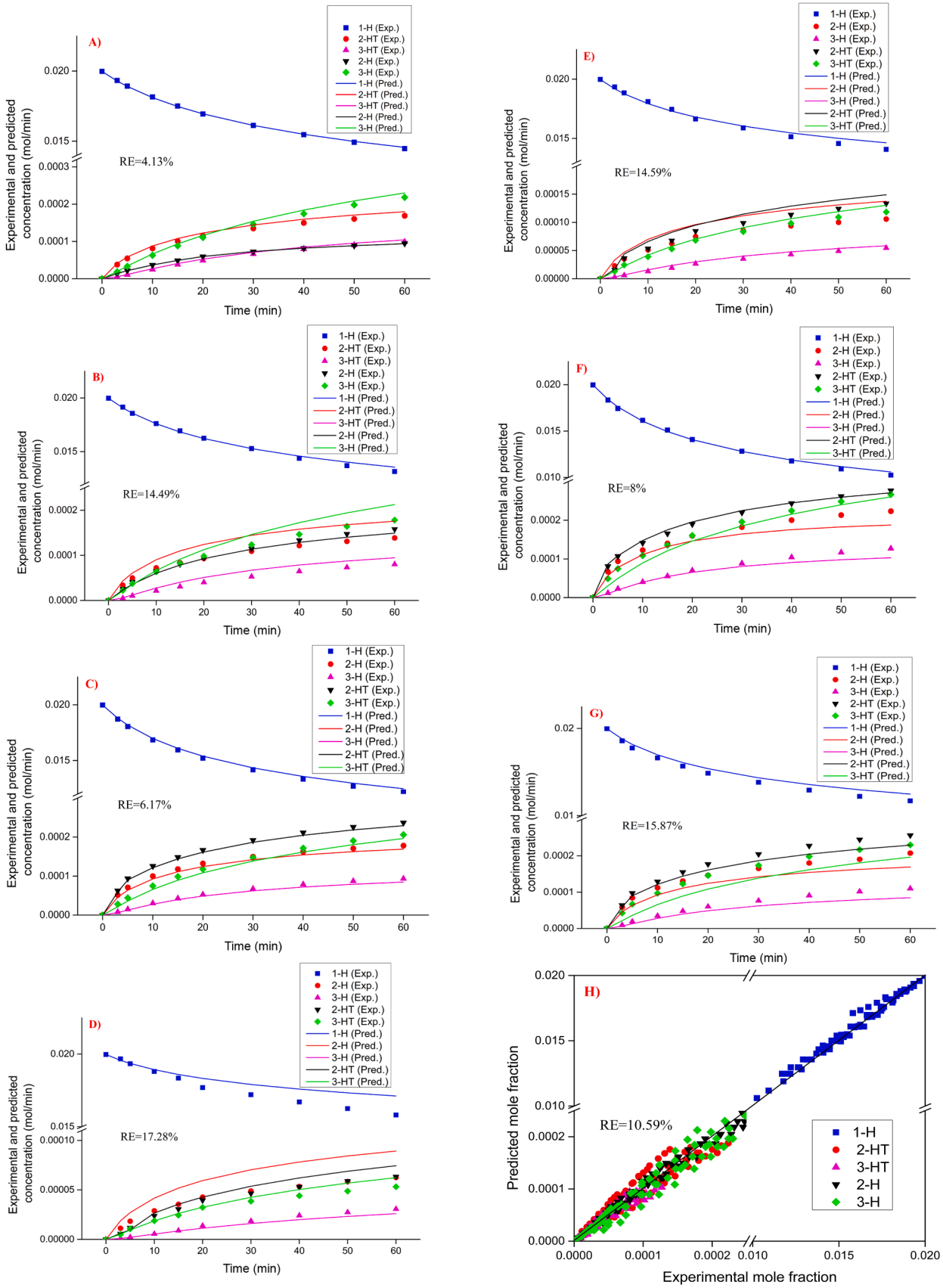

Fig. 15. Comparison of experimental and predicted molar quantity by employing **fresh H-beta** with 0.3 g catalyst weight, 3:1 toluene:hept-1-ene ratio and 60 min reaction time under: **A)** 70, **B)** 80, and **C)** 90 °C reaction temperature. At 90 °C reaction temperature, 3:1 toluene:hept-1-ene ratio and 60 min reaction time using: **D)** 0.1 and **E)** 0.2 g catalyst weight. At 90 °C reaction temperature, 0.3 g catalyst weight, and 60 min reaction time using: **F)** 1:1 and **G)** 2:1 toluene:hept-1-ene ratio. **H)** Comparison of experimental and predicted molar fractions for the entire data.

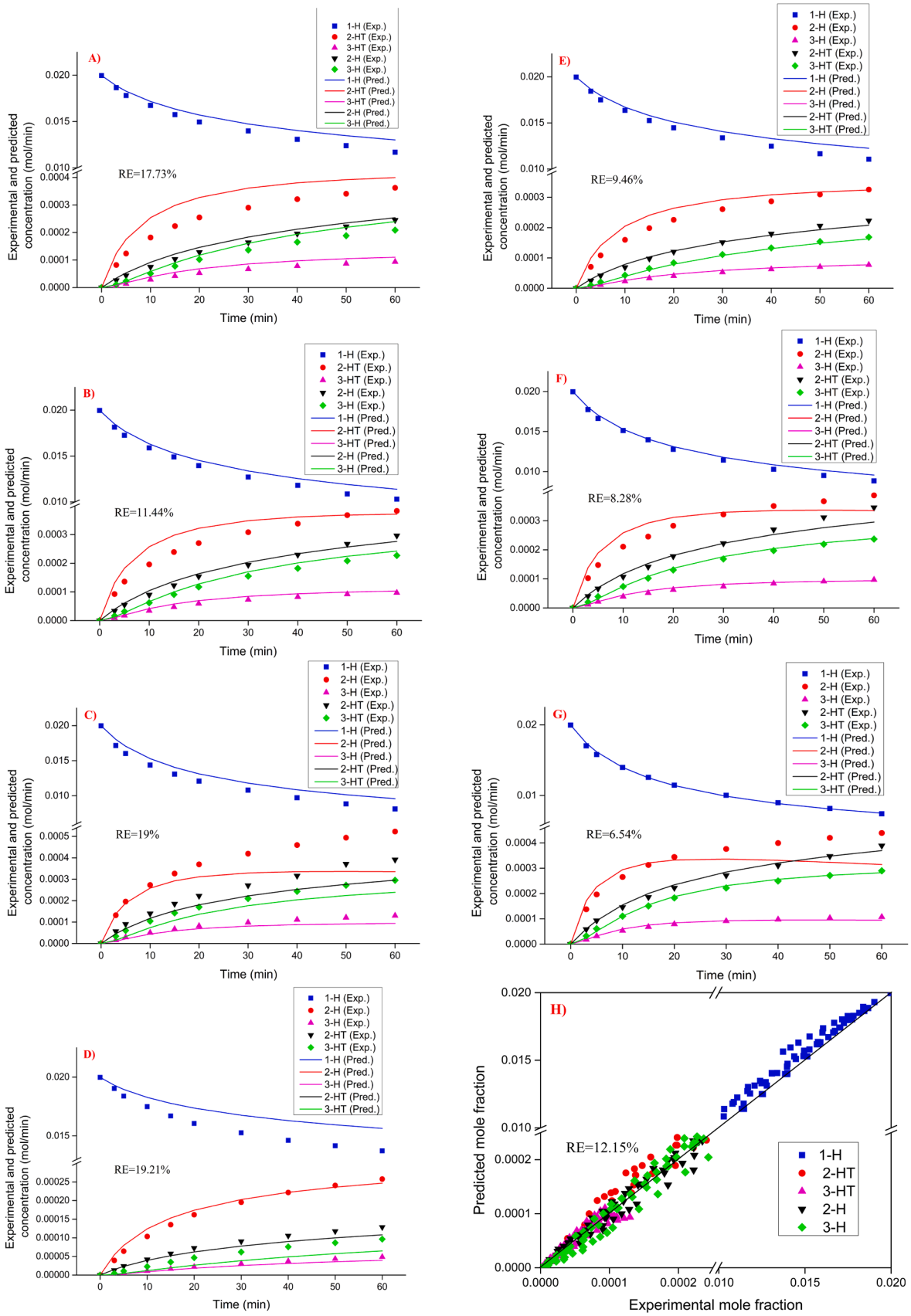

Fig. 16. Comparison of experimental and predicted molar quantity by employing **dealuminated H-beta** with 0.3 g catalyst weight, 3:1 toluene:hept-1-ene ratio and 60 min reaction time under: **A)** 70, **B)** 80, and **C)** 90 °C reaction temperature. At 90 °C reaction temperature, 3:1 toluene:hept-1-ene ratio and 60 min reaction time using: **D)** 0.1 and **E)** 0.2 g catalyst weight. At 90 °C reaction temperature, 0.3 g catalyst weight, and 60 min reaction time using: **F)** 1:1 and **G)** 2:1 toluene:hept-1-ene ratio. **H)** Comparison of experimental and predicted molar fractions for the entire data.

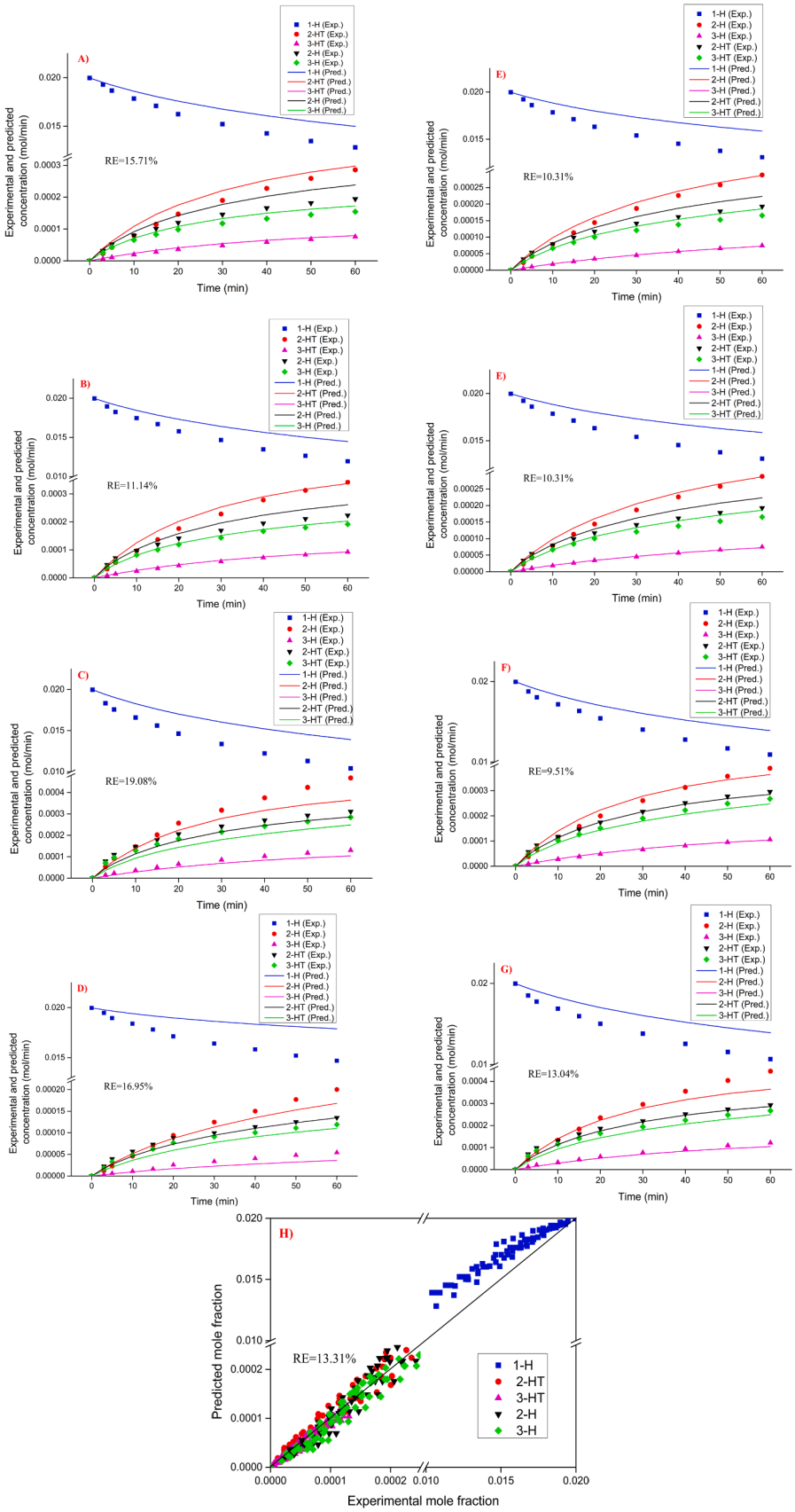

Fig. 17. Comparison of experimental and predicted molar quantity by employing **desilicated H-beta** with 0.3 g catalyst weight, 3:1 toluene:hept-1-ene ratio and 60 min reaction time under: **A)** 70, **B)** 80, and **C)** 90 °C reaction temperature. At 90 °C reaction temperature, 3:1 toluene:hept-1-ene ratio and 60 min reaction time using: **D)** 0.1 and **E)** 0.2 g catalyst weight. At 90 °C reaction temperature, 0.3 g catalyst weight, and 60 min reaction time using: **F)** 1:1 and **G)** 2:1 toluene:hept-1-ene ratio. **H)** Comparison of experimental and predicted molar fractions for the entire data.

Table 4
Activation energy obtained on the surfaces of fresh, dealuminated, and desilicated H-beta zeolite catalysts.

Reaction	Elementary step	*E* (kJ/mol) Fresh H-beta	*E* (kJ/mol) dealuminated H-beta	*E* (kJ/mol) desilicated H-beta
Isomerisation	$1H \rightarrow 2H$	54.8	29.8	27.7
	$2H \rightarrow 1H$	31.5	77.6	58
	$2H \rightarrow 3H$	70.2	34.9	31.8
	$3H \rightarrow 2H$	55	50.5	51.3
Overall		211.5	192.8	168.8
Alkylation	$1H + T \rightarrow 2-HT$	95.1	49	43.1
	$2H + T \rightarrow 2-HT$	42.8	76.8	68.6
	$2H + T \rightarrow 3-HT$	91.1	40.4	40
	$3H + T \rightarrow 2-HT$	122.9	87.1	80.9
Overall		351.9	253.3	170.6
Coking	$1H \rightarrow Coke$	277.2	107.8	104.1
	$2H \rightarrow Coke$	166.6	245.6	231.2
	$3H \rightarrow Coke$	45.8	165.3	158.3
	$2-HT \rightarrow Coke$	63.5	97.3	50.1
	$3-HT \rightarrow Coke$	54.8	50.9	54
Overall		607.9	666.9	597.7

to be approximately 212, 193 and 169 kJ/mol over fresh, dealuminated and desilicated H-beta zeolite catalysts, respectively. The same phenomenon occurred with alkylation reactions, where the overall activation energies decreased after modification of the catalysts compared to the parent sample, from 392 kJ/mol over fresh H-beta surface to 253 and 171 kJ/mol over dealuminated and desilicated zeolite catalysts, respectively.

Moreover, it is noted from the results obtained that the effect of modifying the structures of the catalysts was very clear in improving their catalytic behaviour during the reactions, and the reason for this was either due to an increase in the Si/Al ratio, i.e., a decrease in the acidity of the dealuminated catalyst (see Table 3) or due to the increase in the surface area and pore volume of the desilicated catalyst (see Table 2).

However, the coke products accumulated during the reactions have higher overall activation energies than isomerisation and alkylation reactions. The activation energy on the fresh catalyst surface reached about 608 kJ/mol, while it increased to 667 kJ/mol on the dealuminated catalyst surface and slightly decreased to 598 kJ/mol on the desilicated catalyst surface.

The apparent activation energy (E_a) of isomerisation of hept-1-ene, alkylation of toluene with hept-1-ene, and coke formation were calculated for the purpose of building a clear and comprehensive view to compare the catalytic performance of the catalysts. The apparent activation energies were calculated using Eq. (8) [Al-Iessa and al., 2023, Aslam et al., 2015]. It should be noted that the overall reaction rate constant represents the sum of the rate constants for all parallel reactions, i.e. $K = K_1 + K_2 + \ldots + K_n$. Table 5, a–c illustrates the apparent activation energies of the different reaction groups (i.e., isomerisation, alkylation and coke formation) found at different temperatures on the surfaces of fresh, dealuminated, and desilicated H-beta zeolite catalysts.

$$E_a = \frac{E_1K_1 + E_2K_2 + \ldots + E_nK_n}{K_1 + K_2 + \ldots + K_n} \quad (8)$$

As a general rule, lower levels of apparent activation energies at three different reaction temperatures were identified for isomerisation and alkylation reactions on the surface of the modified catalysts in comparison with the values obtained on the surface of fresh catalyst. On the contrary, the apparent activation energy values increase for the coke formation reaction on the surface of the modified catalysts compared to the values obtained on the surface of the fresh catalyst. In fact, the lowest values of apparent activation energies were found on the surface of dealuminated and desilicated H-beta catalysts for the isomerisation and coke formation reactions at 70 °C, while the apparent activation energy values for the alkylation reaction seemed to be unaffected by the reaction temperatures. This indicates that isomerisation reactions are more active at low reaction temperature (i.e., 70 °C), with less coke being deposited on the catalyst surface, and without any significant effect on the pathway of alkylation reactions. The apparent activation energy of toluene alkylation reactions with hept-1-ene on the surfaces of the three catalysts used in this study at temperatures ranging from 70 to 90 °C was found to be between 40 and 90 kJ/mol. These values are fairly close to what has been reported in similar studies in the published. In most of these previous kinetic studies, apparent activation energies were calculated according to some assumptions. Yadav and Doshi [Yadav and Doshi, 2002], Tsai et al. [Tsai et al., 2003] and de Almeida et al. [de Almeida et al., 1994], studied the alkylation of benzene with dode-1-cene on non-zeolite, mordenite, and Y zeolite catalysts, and found that the activation energies of the alkylation are approximately 85, 70, and 63 kJ/mol, respectively. Corma et al. [Corma et al., 2000] and Craciun et al. [Craciun et al., 2012] studied the kinetics of benzene alkylation with propene and oct-1-ene, and obtained activation energies of 77 and 46 kJ/mol, respectively. Aslam et al. [Aslam et al., 2015] found that the activation energy of dode-1-cene isomerisation was 34 kJ/mol for 1- to dode-2-cene, while it was about 50 kJ/mol for 2- to dode-3-cene. In addition, they measured the activation energies of the alkylation reactions of 2- and 3-phenyldodecene, and they were about 49 and 66 kJ/mol, respectively. Finally, the resulting data and parameters showed that the activation energies for the categories of such a complex reaction increase in the following order: double bond isomerisation < oligomerisation < alkylation, according to the study conducted by [Cowley et al., 2005].

Tables 6,7

In addition, as shown in Fig. 18, the highest apparent activation energy for the coke formation reaction calculated on the surface of the catalyst with the lowest Si/Al ratio (i.e., after the desilication treatment) at three different reaction temperatures and this is in agreement with the results obtained by the TGA analyser in Fig. 9. This can be explained by the fact that the presence of acidic sites associated with aluminium atoms, along with the decrease in the number of silicon atoms after treatment, simultaneously with the increase in surface area and pore volume, helped to make the surface of this catalyst more acidic and more stimulating the formation of coke on its surface.

Table 5-a
Calculated values of apparent activation energies at 90 °C.

	Elementary step	E_a (kJ/mol) Fresh H-beta (Si/Al = 367)	E_a (kJ/mol) dealuminated H-beta (Si/Al = 563)	E_a (kJ/mol) desilicated H-beta (Si/Al = 231)
1	Isomerisation	52.8	38.5	39.9
2	Alkylation	91	40.4	68.6
3	Coking	45.8	50.9	147.3

Table 5-b
Calculated values of apparent activation energies at 80 °C.

	Elementary step	E_a (kJ/mol) Fresh H-beta (Si/Al = 367)	E_a (kJ/mol) dealuminated H-beta (Si/Al = 563)	E_a (kJ/mol) desilicated H-beta (Si/Al = 231)
1	Isomerisation	52.5	38.1	38.9
2	Alkylation	91	40.4	68.6
3	Coking	45.8	50.9	132.7

Table 5-c
Calculated values of apparent activation energies at 70 °C.

	Elementary step	E_a (kJ/mol) Fresh H-beta (Si/Al = 367)	E_a (kJ/mol) dealuminated H-beta (Si/Al = 563)	E_a (kJ/mol) desilicated H-beta (Si/Al = 231)
1	Isomerisation	52	37.6	37.8
2	Alkylation	90.9	40.4	68.6
3	Coking	45.8	48.9	107

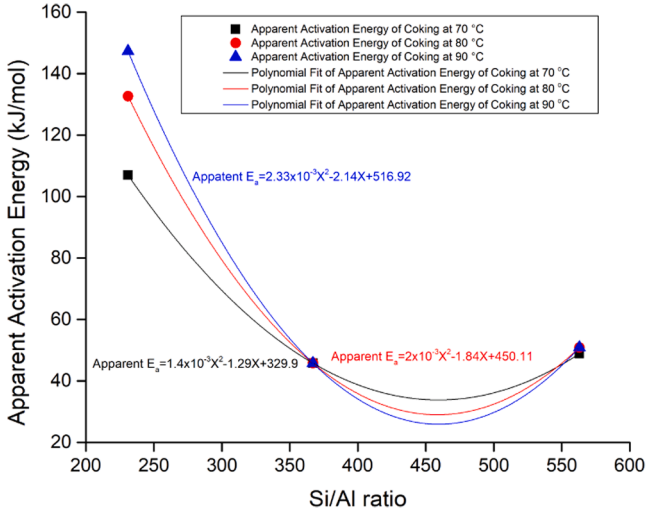

Fig. 18. The relationship of the Si/Al ratio of catalysts with the apparent activation energy values of coke formation reactions at 70, 80, and 90 °C.

4. Conclusion

Acid leaching and base leaching methods were successfully utilized to treat the structural framework of H-beta zeolite according to the analysis results obtained from deferent characterisation techniques. Compared to the parent sample, it was observed that the desilicated H-beta sample showed an obvious decrease in the degree of crystallinity coinciding with a decrease in ICP-Si/Al with an increase in surface area and pore volume. While, on the contrary, an increase in the degree of crystallinity, as well as an increase in the ICP-Si/Al, with a decrease in the surface area and pore volume were found in the Dealuminated H-beta sample. The catalytic behaviour of the parent catalyst and the modified catalysts in n-heptane alkylation reactions using toluene was compared, and the effect of different reaction conditions, which included temperature, toluene to heptane ratio and catalyst weight, on the reactants and products distribution was studied experimentally. In general, the results on both types of modified catalysts indicate an improvement in the conversion of double-bond isomerisation and alkylation products with a significant reduction in the amount of deposited coke compared to the results on the fresh catalyst, especially when the toluene: Hept-1-ene ratio is 3:1 (i.e., increased the amount of catalyst used to 0.3 g). It was also found that 60 min is the preferred reaction time and 90 °C appears to be the most suitable for this type of exothermic reaction over the surfaces of the three catalysts with different Si/Al ratios (i.e. fresh (367), dealuminated (563) and desilicated (231). Furthermore, the seven-component reaction scheme and thirteen reactions were applied in kinetic modelling to fit the experimental data. It was found that the predicted concentrations agree well with the experimental data, providing evidence of the validity of the kinetic model and the proposed reaction scheme. After conducting a combination of nonlinear differential equation solving technique and nonlinear regression analysis technique, it was found that the overall activation energies on the surfaces of the three catalysts used are in the range 168.8–211.5 kJ/mol for isomerisation reactions, 170.6–351.9 kJ/mol for alkylation reactions, and 597.7–666.9 kJ/mol for coke formation reactions. Finally, through calculations of the apparent activation energies of the estimated reaction steps, it was found that isomerisation reactions have the lowest apparent activation energy, that is, the lowest reaction barrier on the surfaces of the modified catalysts. processing and potential to mix totally with aqueous solutions.

Declaration

Funding

Not applicable.

Data availability statement

The data that has been used is confidential.

Consent for publication

Not applicable.

Ethics approval and consent to participate

Not applicable.

CRediT authorship contribution statement

Ali Al-Shathr: Conceptualization, Methodology, Software, Writing – review & editing. **Bashir Y. Al-Zaidi:** Writing – review & editing, Conceptualization, Methodology, Software. **Safa Aal-Kaeb:** Conceptualization, Methodology, Software. **Zaidoon M. Shakor:** Conceptualization, Methodology, Software. **Hasan Sh. Majdi:** Visualization, Investigation. **May A. Alsaffar:** Visualization, Investigation. **Muhannad A.E. Al-Saedy:** Visualization, Investigation. **Ahmed Majeed Jassem:** Supervision. **Ramzy S. Hamied:** Software, Validation. **Firas K. Al-Zuhairi:** Software, Validation. **Adnan A. AbdulRazak:** Software, Validation. **Talib M. Albayati:** Writing – review & editing, Visualization, Writing – original draft. **James McGregor:** Writing – review & editing.

Declaration of competing interest

The authors declare that they have no known competing financial interests or personal relationships that could have appeared to influence the work reported in this paper.

Acknowledgement

The authors are grateful to the Chemical Engineering Department, University of Technology, Baghdad, Iraq, and Doctor Alan Dunbar (Chemical and Biological Engineering department, the University of Sheffield) is thanked for his contribution to obtain the SEM results.

References

Abood, E.A., et al., 2024. Machine Learning-Based Prediction Models for Punching Shear Strength of Fiber-Reinforced Polymer Reinforced Concrete Slabs Using a Gradient-Boosted Regression Tree 17 (16), 3964.
Adriano, A., et al., 2022. Dealumination and Characterization of Natural Mordenite-Rich Tuffs. Materials. (Basel) 15 (13).
Ali, N.S., et al., 2023. Utilization of Loaded Cobalt onto MCM-48 Mesoporous Catalyst as a Heterogeneous Reaction in a Fixed Bed Membrane Reactor to Produce Isomerization Product from n-Heptane 13 (7), 1138.
Al-Iessa, M.S., et al., 2023. Optimization of Polypropylene Waste Recycling Products as Alternative Fuels through Non-Catalytic Thermal and Catalytic Hydrocracking Using Fresh and Spent Pt/Al2O3 and NiMo/Al2O3 Catalysts 16 (13), 4871.
Aliyeva, R.V., et al., 2021. The alkylation of oil fractions rich in aromatic hydrocarbons with C6, C8 and C10 α - olefins in the presence of ionic liquids catalytic systems. Appl. Petrochem. Res. 11 (1), 65–77.

Alsaadi, M., et al., 2025. Logical reasoning for human activity recognition based on multisource data from wearable device. Sci. Rep. 15 (1), 380.
Alsaadi, M., Seno, M., Khalaf, M., 2024. Internet of Things Software Engineering Model Validation Using Knowledge-Based Semantic Learning. Intelligent Automation & Soft Computing 40, 1–10.
Al-Shathr, A., et al., 2021. Comparison between Artificial Neural Network and Rigorous Mathematical Model in Simulation of Industrial Heavy Naphtha Reforming Process 11 (9), 1034.
Al-Shathr, A., et al., 2022. Reaction Kinetics of Cinnamaldehyde Hydrogenation over Pt/SiO_2: Comparison between Bulk and Intraparticle Diffusion Models. International Journal of Chemical Engineering 2022, 8303874.
Al-Shathr, A., et al., 2023. Experimental and kinetic studies of the advantages of coke accumulation over Beta and Mordenite catalysts according to the pore mouth catalysis hypothesis. Catal. Commun. 181, 106718.
Al-Sultani, S.H., Al-Shathr, A., Al-Zaidi, B.Y., 2024. Aromatics Alkylated with Olefins Utilizing Zeolites as Heterogeneous Catalysts: A Review 5 (4), 900–927.
Al-Sultani, S.H., Al-Shathr, A., Al-Zaidi, B.Y., 2024. Toluene Alkylation Reactions over Y-Type Zeolite Catalysts: An Experimental and Kinetic Study 5 (4), 1042–1065.
Altındaş, C., et al., 2023. Synergistic interaction of metal loaded multifactorial nanocatalysts over bifunctional transalkylation for environmental applications. Environ. Res. 216, 114479.
Al-Zaidi, B.Y., et al., 2023. Hydroisomerisation and Hydrocracking of n-Heptane: Modelling and Optimisation Using a Hybrid Artificial Neural Network–Genetic Algorithm (ANN–GA) 13 (7), 1125.
Al-Zaidi, B.Y., Holmes, R.J., Garforth, A.A., 2012. Study of the Relationship between Framework Cation Levels of Y Zeolites and Behavior during Calcination, Steaming, and n-Heptane Cracking Processes. Ind. Eng. Chem. Res. 51 (19), 6648–6657.
Aslam, W., et al., 2014. Selective synthesis of linear alkylbenzene by alkylation of benzene with 1-dodecene over desilicated zeolites. Catal. Today 227, 187–197.
Aslam, W., et al., 2015. Kinetics modeling of liquid phase alkylation of benzene with dodecene over mordenite 93.
Aziz, I., et al., 2023. Effect of desilication process on natural zeolite as Ni catalyst support on hydrodeoxygenation of palm fatty acid distillate (PFAD) into green diesel. S. Afr. J. Chem. Eng. 45, 328–338.
Azzolina Jury, F., et al., 2013. Synthesis and characterization of MEL and FAU zeolites doped with transition metals for their application to the fine chemistry under microwave irradiation. Applied Catalysis A: General 453, 92–101.
Barakov, R., et al., 2022. Hierarchical Beta Zeolites As Catalysts in α-Pinene Oxide Isomerization. ACS. Sustain. Chem. Eng. 10, 6642–6656. American Chemical Society.
Bolshakov, A., et al., 2020. Hierarchically porous FER zeolite obtained via FAU transformation for fatty acid isomerization. Applied Catalysis B: Environmental 263, 118356.
Boveri, M., et al., 2006. Steam and acid dealumination of mordenite: Characterization and influence on the catalytic performance in linear alkylbenzene synthesis. Catal. Today 114 (2), 217–225.
Busca, G., 2014. Heterogeneous Catalytic Materials. Elsevier, Amsterdam.
Cadenas, M., et al., 2014. Alkylation of toluene with 1-hexene over macroreticular ion-exchange resins. Applied Catalysis A: General 485, 143–148.
Chalupka, K., et al., 2018. Dealuminated Beta Zeolite Modified by Alkaline Earth Metals. J. Chem. 2018, 7071524.
Chaurasia, V., et al., 2022. Self-care, Household Cleaning and Disinfection During COVID-19 Pandemic: a Study from Metropolitan Cities of India. Annals of Data Science 9 (5), 1085–1101.
Contrera, R.C., et al., 2014. First-order kinetics of landfill leachate treatment in a pilot-scale anaerobic sequence batch biofilm reactor. J. Environ. Manage 145, 385–393.
Corma, A., Martínez-Soria, V., Schnoeveld, E., 2000. Alkylation of Benzene with Short-Chain Olefins over MCM-22 Zeolite: Catalytic Behaviour and Kinetic Mechanism. J. Catal. 192 (1), 163–173.
Cowley, M., de Klerk, A., Nel, R.J.J., 2005. Amylation of Toluene by Solid Acid Catalysis. Ind. Eng. Chem. Res. 44 (15), 5535–5541.
Craciun, I., Reyniers, M.F., Marin, G.B., 2012. Liquid-phase alkylation of benzene with octenes over Y zeolites: Kinetic modeling including acidity descriptors. J. Catal. 294, 136–150.
Da, Z., et al., 2001. Liquid-phase alkylation of toluene with long-chain alkenes over HFAU and HBEA zeolites. Applied Catalysis A: General 219 (1–2), 45–52.
de Almeida, J.G., et al., 1994. Effect of pore size and aluminium content on the production of linear alkylbenzenes over HY, H-ZSM-5 and H-ZSM-12 zeolites: Alkylation of benzene with 1-dodecene. Applied Catalysis A: General 114 (1), 141–159.
Deshmukh, A.A., et al., 2024. Trusted Personalized and Contextualized E-Commerce Services for Consumer Electronics over Wireless Sensor Network. IEEE Transactions on Consumer Electronics, p. 1-1.
Díaz, M., et al., 2021. Coke deactivation and regeneration of HZSM-5 zeolite catalysts in the oligomerization of 1-butene. Applied Catalysis B: Environmental 291, 120076.
Faghihian, H., Mohammadi, M.H., 2012. A novel catalyst for alkylation of benzene. Comptes Rendus Chimie 15 (11), 962–968.
Feng, L., et al., 2017. Application of the Initial Rate Method in Anaerobic Digestion of Kitchen Waste. Biomed. Res. Int. 2017, 3808521.
Gomez, L.Q., et al., 2020. H2-free Synthesis of Aromatic, Cyclic and Linear Oxygenates from CO2 13 (3), 647–658.
Guisnet, M., 2002. Coke" molecules trapped in the micropores of zeolites as active species in hydrocarbon transformations. Journal of Molecular Catalysis A: Chemical 367–382, 182–183.
Gunnoe, T.B., et al., 2020. Transition-Metal-Catalyzed Arene Alkylation and Alkenylation: Catalytic Processes for the Generation of Chemical Intermediates. ACS. Catal. 10 (23), 14080–14092.
Han, S., et al., 2022. Cooperative Surface Passivation and Hierarchical Structuring of Zeolite Beta Catalysts 61 (41), e202210434.
Holland, J.H., 1975. Adaptation in natural and artificial systems.
Hong, L., et al., 2023. Research Progress on the Synthesis of Nanosized and Hierarchical Beta Zeolites 11 (5), 214.
Horňáček, M., et al., 2009. Alkylation of Benzene with 1-Alkenes over Zeolite Y and Mordenite. Acta Chimica Slovaca 2 (1), 31–45.
Ilcheva, V., et al., 2024. Effect of Gadolinium Doping on the Structure of Ce1-xGdxO2-x/2 Solid Solutions Prepared by Ionic Gelation Approach. Emerging Science Journal 8, 1686–1696.
Imyen, T., et al., 2020. Tailoring hierarchical zeolite composites with two distinct frameworks for fine-tuning the product distribution in benzene alkylation with ethanol. Nanoscale Adv. 2 (10), 4437–4449.
Intang, A., et al., 2024. Determination of swelling operation parameters to improve the hierarchy of natural zeolite Lampung after synthesis. S. Afr. J. Chem. Eng. 50, 125–134.
Jae, J., et al., 2011. Investigation into the shape selectivity of zeolite catalysts for biomass conversion. J. Catal. 279 (2), 257–268.
Klunk, M.A., et al., 2020. Synthesis and characterization of mordenite zeolite from metakaolin and rice husk ash as a source of aluminium and silicon. Chemical Papers 74 (8), 2481–2489.
Kocal, J.A., Vora, B.V., Imai, T., 2001. Production of linear alkylbenzenes. Applied Catalysis A: General 221 (1–2), 295–301.
Krisnandi, Y.K., et al., 2019. Synthesis and Characterization of Crystalline NaY-Zeolite from Belitung Kaolin as Catalyst for n-Hexadecane Cracking 9 (8), 404.
Lee, S.U., et al., 2023. Compositional dependence of Co- and Mo-supported beta zeolite for selective one-step hydrotreatment of methyl palmitate to produce bio jet fuel range hydrocarbons. RSC. Adv. 13 (3), 2168–2180.
Li, J., et al., 2017. Carboxylic acids to butyl esters over dealuminated–realuminated beta zeolites for removing organic acids from bio-oils. RSC. Adv. 7 (54), 33714–33725.
Li, J., et al., 2023. Regulation of the Si/Al ratios and Al distributions of zeolites and their impact on properties. Chem. Sci. 14 (8), 1935–1959.
Li, Q., et al., 2017. Wettable magnetic hypercrosslinked microporous nanoparticle as an efficient adsorbent for water treatment. Chemical Engineering Journal 326, 109–116.
Li, X., Prins, R., van Bokhoven, J.A., 2009. Synthesis and characterization of mesoporous mordenite. J. Catal. 262 (2), 257–265.
Liu, Z., et al., 2022. Seeds induced Beta zeolite synthesis with low SDA for n-heptane catalytic cracking reaction. Catal. Today 235–241, 405-406.
Lovás, P., et al., 2014. Preparation of an active and regenerable catalyst for liquid-phase alkylation of toluene with 1-decene. Applied Catalysis A: General 475, 341–346.
Lu, W., et al., 2021. Synthesis of Linear Alkylbenzenes over Beta Zeolites with Enhanced Transport and Surface Activity. Industrial & Engineering Chemistry Research, 60 (33), 12275–12281.
Lutz, W., et al., 2000. Phase Transformations in Alkaline and Acid Leached Y Zeolites Dealuminated by Steaming 626 (6), 1460–1467.
Magnoux, P., et al., 1997. Influence of the acidity and of the pore structure of zeolites on the alkylation of toluene by 1-heptene. In: Blaser, A.B.H.U., Prins, R. (Eds.), Studies in Surface Science and Catalysis. Elsevier, pp. 107–114. Editors.
Mendoza Merlano, C.J., et al., 2022. Effect of crystal size on the acidity of nanometric Y zeolite: number of sites, strength, acid nature, and dehydration of 2-propanol. New Journal of Chemistry.
Minami, A., et al., 2022. Ultrafast dealumination of *BEA zeolite using a continuous-flow reactor. Advanced Powder Technology 33 (8), 103702.
Mintova, S., et al., 2006. Variation of the Si/Al ratio in nanosized zeolite Beta crystals. Microporous and Mesoporous Materials 90 (1), 237–245.
Moljord, K., Magnoux, P., Guisnet, M., 1995. Coking, aging and regeneration of zeolites XV. Influence of the composition of HY zeolites on the mode of formation of coke from propene at 450°C. Applied Catalysis A: General 122 (1), 21–32.
Mordor-Intelligence, 2023. Linear Alkyl Benzene (LAB) Market. India.
Mulakhudair, A.R., et al., 2023. Assessment of the Correlation Between Inflammatory Status and Severity of COVID-19: Experience from Tertiary Hospital in Iraq. Curr. Microbiol. 80 (9), 283.
Müller, M., Harvey, G., Prins, R., 2000. Comparison of the dealumination of zeolites beta, mordenite, ZSM-5 and ferrierite by thermal treatment, leaching with oxalic acid and treatment with SiCl4 by 1H, 29Si and 27Al MAS NMR. Microporous and Mesoporous Materials 34 (2), 135–147.
Narayanan, S., et al., 2015. Characterization and catalytic reactivity of mordenite – Investigation of selective oxidation of benzyl alcohol. Polyhedron. 89, 289–296.
Nisar, N., et al., 2024. Novel Ni/ZnO Nanocomposites for the Effective Photocatalytic Degradation of Malachite Green Dye. Civil Engineering Journal 10, 2601–2614.
Pérez-Guevara, E., et al., 2020. Study by NMR of Liquid-Phase Alkylation of Toluene with Hex-1-ene: Effect of Catalyst on Selectivity. Petroleum Chemistry 60 (7), 810–817.
Perez-Sena, W.Y., et al., 2021. Use of semibatch reactor technology for the investigation of reaction mechanism and kinetics: Heterogeneously catalyzed epoxidation of fatty acid esters. Chem. Eng. Sci. 230, 116206.
Přech, J., et al., 2018. From 3D to 2D zeolite catalytic materials. Chem. Soc. Rev. 47 (22), 8263–8306.
Qi, J., et al., 2018. The reactions that determine the yield and selectivity of 1,3,5-trioxane. Chemical Engineering Journal 331, 311–316.
Quintana-Gómez, L., et al., 2022. Reverse combustion" of carbon dioxide in water: The influence of reaction conditions. Front. Energy Res. 10, 917943.

Saleh, N.J., Al-Zaidi, B.Y.S., Sabbar, Z.M., 2018. A Comparative Study of Y Zeolite Catalysts Derived from Natural and Commercial Silica: Synthesis, Characterization, and Catalytic Performance. Arab. J. Sci. Eng. 43 (11), 5819–5836.
Shakor, Z., Abdulrazak, A., Sukkar, K., 2020. A Detailed Reaction Kinetic Model of Heavy Naphtha Reforming. Arab. J. Sci. Eng. 45, 7361–7370.
Shakor, Z., Shafei, E., 2023. The mathematical catalyst deactivation models: a mini review. RSC. Adv. 13, 22579–22592.
Shakor, Z.M., AbdulRazak, A.A., Shuhaib, A.A., 2021. Optimization of process variables for hydrogenation of cinnamaldehyde to cinnamyl alcohol over a Pt/SiO2 catalyst using response surface methodology. Chem. Eng. Commun. 1–17.
Shakor, Z.M., Ramos, M.J., AbdulRazak, A.A., 2022. A detailed reaction kinetic model of light naphtha isomerization on Pt/zeolite catalyst. Journal of King Saud University - Engineering Sciences 34 (5), 303–308.
Siffert, S., Gaillard, L., Su, B.L., 2000. Alkylation of benzene by propene on a series of Beta zeolites: toward a better understanding of the mechanisms. Journal of Molecular Catalysis A: Chemical 153 (1), 267–279.
Silaghi, M.C., Chizallet, C., Raybaud, P., 2014. Challenges on molecular aspects of dealumination and desilication of zeolites. Microporous and Mesoporous Materials 191, 82–96.
Silva, L., et al., 2019. Desilication of ZSM-5 and ZSM-12 Zeolites with Different Crystal Sizes: Effect on Acidity and Mesoporous Initiation. Materials Research 22.
Singh, B.K., et al., 2021. Synthesis of Mesoporous Zeolites and Their Opportunities in Heterogeneous Catalysis 11 (12), 1541.
Sohn, J.R., et al., 1986. Determination of framework aluminium content in dealuminated Y-type zeolites: a comparison based on unit cell size and wavenumber of i.r. bands. Zeolites 6 (3), 225–227.
Struebing, H., et al., 2013. Computer-aided molecular design of solvents for accelerated reaction kinetics. Nat. Chem. 5 (11), 952–957.
Tsai, T.C., et al., 2003. Development of a green LAB process: alkylation of benzene with 1-dodecene over mordenite. Green Chemistry 5 (4), 404–409.
van Vreeswijk, S.H., et al., 2023. Micro- and Nanoscale Heterogeneities in Zeolite Beta as Measured by Atom Probe Tomography and Confocal Fluorescence Microscopy 24 (13), e202300094.
Visan, A., et al., 2019. Photocatalytic Reactor Design: Guidelines for Kinetic Investigation. Ind. Eng. Chem. Res. 58 (14), 5349–5357.
Vogt, C., Weckhuysen, B.M., 2022. The concept of active site in heterogeneous catalysis. Nature Reviews Chemistry 6 (2), 89–111.
Wang, B., Manos, G., 2007. A novel thermogravimetric method for coke precursor characterisation. J. Catal. 250 (1), 121–127.
Wang, S., et al., 2023. Catalytic production of 1,2-propanediol from sucrose over a functionalized Pt/deAl-beta zeolite catalyst. RSC Advances, 13 (1), 734–741.
Wang, Y., et al., 2016. Effects of Dealumination and Desilication of Beta Zeolite on Catalytic Performance in n-Hexane Cracking. Catalysts. 6 (1), 8.
Wang, Y., et al., 2022. Mesoporogen-free synthesis of single-crystalline hierarchical beta zeolites for efficient catalytic reactions. Inorg. Chem. Front. 9 (11), 2470–2478.
Wei, Q., et al., 2019. Citric Acid-Treated Zeolite Y (CY)/Zeolite Beta Composites as Supports for Vacuum Gas Oil Hydrocracking Catalysts: High Yield Production of Highly-Aromatic Heavy Naphtha and Low-BMCI Value Tail Oil 7.
Yadav, G.D., Doshi, N.S., 2002. Synthesis of Linear Phenyldodecanes by the Alkylation of Benzene with 1-Dodecene over Non-Zeolitic Catalysts. Org. Process. Res. Dev. 6 (3), 263–272.
Yoshioka, T., et al., 2022. Dealumination of small-pore zeolites through pore-opening migration process with the aid of pore-filler stabilization. Sci. Adv. 8 (25), eabo3093.
Yuan, B., et al., 2023. Deactivation Mechanism and Anti-Deactivation Measures of Metal Catalyst in the Dry Reforming of Methane: A Review 14 (5), 770.
Yuan, X.D., et al., 2002. Alkylation of benzene with 1- dodecene over usy zeolite catalyst: Effect of pretreatment and reaction conditions. Korean Journal of Chemical Engineering 19 (4), 607–610.
Zaykovskaya, A.O., et al., 2020. Synthesis and physico-chemical characterization of Beta zeolite catalysts: Evaluation of catalytic properties in Prins cyclization of (−)-isopulegol. Microporous and Mesoporous Materials 302, 110236.
Zhang, K., et al., 2018. Organotemplate-free synthesis of hierarchical beta zeolites. Catal. Today 316, 26–30.
Zhang, K., et al., 2018. Organotemplate-Free β Zeolites: From Zeolite Synthesis to Hierarchical Structure Creation. ACS Omega, 3 (12), 18935–18942.
Zhang, W., et al., 2018. A Feasible One-Step Synthesis of Hierarchical Zeolite Beta with Uniform Nanocrystals via CTAB 11 (5), 651.